

Congested Crossing Pedestrian Traffic Flow : Dispersion vs. Transport in Crowded Areas

Mariam Al Khatib[‡], Said Gounane[†], Nouredine Igbida[‡], and Ghadir Jradi[‡]

ABSTRACT. This study investigates the complex dynamic interactions between two typed populations coexisting within a shared space. We propose both theoretical and numerical study to analyze scenarios where one population (population 1) must traverse a territory occupied by another (population 2), necessitating strategies to mitigate overcrowding caused by spatial limitations. To capture these interactions, we model population 1 using a linear transport equation, while population 2 is described by a granular diffusion model à la sandpile to represent its internal dynamics and tendency to decongest. Through numerical simulations, we explore how different movement strategies of the traversing population (population 1) – including directed motion towards a specific destination, internal dispersion to minimize crowding, and uniform dispersal across the space – affects the behavior of population 2.

keywords: Crowded motion; congestion, transport equation, 1–Wasserstein distance, W_1 –gradient flow, minimum-flow problem, primal-dual numerical optimization.

AMS Subject Classification: 22E46, 53C35, 57S20.

1. Introduction

Consider two distinct populations ρ_1 and ρ_2 , occupying a common space, denoted by Ω . Population ρ_1 must traverse an area inhabited by ρ_2 requiring a strategic interaction to manage congestion. Given the limited spatial capacity, the dynamic interplay between these populations can easily lead to congestion.

In this paper, we develop a macroscopic mathematical model for these congested pedestrian flows. By treating the crowd as a collective entity, we can apply this approach to

[‡]Institut de recherche XLIM-DMI, UMR-CNRS 6172, Faculté des Sciences et Techniques, Université de Limoges, France. Emails: noureddine.igbida@unilim.fr, mariam.al_khatib@unilim.fr.

[†]MIMSC Laboratory, Higher School of Technology Essaouira, Morocco. Emails: s.gounane@uca.ac.ma.

[‡]GJ began this research project while completing her doctoral thesis. She is currently working on it independently, unaffiliated with any institution, ghadirjradi@gmail.com.

large-scale crowd dynamics. Building upon previous works ([9, 25, 26]), we use the continuity equation to describe the macroscopic dynamics of each population:

$$\partial_t \rho_i + \nabla \cdot (\rho_i U_i) = 0, \quad \text{for } i = 1, 2,$$

where $\rho_i = \rho_i(t, x)$ represents the density of individuals at time $t \geq 0$ and position $x \in \Omega \subset \mathbb{R}^N$ ($N = 2$), assumed to be a bounded and regular domain. The dynamic of each ρ_i must ensure an admissible global distribution of the population :

$$0 \leq \rho_1 + \rho_2 \leq \rho_{max},$$

where ρ_{max} a given maximum density (assumed to be known). Without loss of generality, we assume throughout the paper that

$$\rho_{max} = 1.$$

Determining the flow velocity vector field U_i remains a challenging task, in general. Although various approaches have been explored, a universal solution is elusive. Balancing the general behavior of the crowd with the behavior of the individual pedestrians is critical. Our approach assumes that while ρ_1 moves toward a fixed target, ρ_2 can adjust its movement based on the instantaneous distribution of both populations. For example, assuming that $U_1 = V$ is a known spontaneous velocity field, we assume that U_2 is a vector field that performs the patch for the spontaneous dynamic when the pedestrian ρ_2 is hindered by the other one. We propose to consider a dynamic vector field U_2 in congested regions given by :

$$U_2 = U_2[\nabla p],$$

where p is a Lagrange multiplier associated with the constraint $0 \leq \rho_1 + \rho_2 \leq \rho_{max} : p \geq 0$ and $p(\rho_{max} - \rho_1 - \rho_2) = 0$. This model ensures that $\rho_1 + \rho_2$ does not exceed ρ_{max} and provides a framework for analyzing the dynamics of these two populations in congested environments.

Inspired by [21], we introduce a grain-like motion velocity field sandpile to model the random microscopic movements of ρ_2 agents, facilitating the passage of ρ_1 while adhering to spatial distribution constraints. More precisely, while the population ρ_1 follows the transport equation

$$(1.1) \quad \partial_t \rho_1 + \nabla \cdot (\rho_1 V) = 0, \quad \text{in } Q := (0, T) \times \Omega,$$

with $\rho_1(0) = \rho_{01}$, we propose to handle the dynamic of the second population ρ_2 , by using the nonlinear second order equation where $\rho_2 = \rho_{max} - \rho_1$ workout the utmost distribution of the population in Ω :

$$(1.2) \quad \begin{cases} \frac{d\rho_2}{dt} + \partial \mathbb{H}_{\text{Lip}_1}(p) = 0 \\ 0 \leq m, p \geq 0, 0 \leq \rho_2 \leq \rho_{max} - \rho_1, p(\rho_{max} - \rho_1 - \rho_2) = 0 \end{cases}$$

with $\rho_2(0) = \rho_{02}$, where $\partial \mathbb{H}_{\text{Lip}_1}$ is the subdifferential of the indicator function of Lip_1 , the set of 1-Lipschitz continuous function.

While the natural boundary condition for the transport equation (1) incorporates the normal trace of the velocity field V (assumed to be known), we examine the dynamics governed by (1) under Neumann boundary conditions. However, (1) still requires Dirichlet boundary conditions on portions of the boundary where V points inward.

The model’s adaptability to various practical scenarios is a key feature. The present paper focuses on a scenario in which only the population ρ_2 experiences congestion, with a priority placed on the movement of ρ_1 . However, the framework can be extended to model situations in which both populations exhibit congestion and transport behaviors. This type of coupled system has been explored theoretically in [28]. The model presented here specifically describes the dynamics of two populations: one with a primary objective (e.g., emergency evacuation) and another that adapts to facilitate the first’s passage while maintaining acceptable density. We conducted an analysis of various transportation types for ρ_1 : (1) directed movement towards a goal, modeled by a velocity field V derived from an eikonal equation; (2) motion influenced by local average density, modeled by a nonlocal potential for V , and also motion inspired by the Keller-Segel models, where the potential is determined by a diffusion equation associated with ρ_2 .

To our knowledge, this study is the first to address congestion within this specific context. While research on cross-diffusion systems, where populations exhibit behaviors to alleviate overcrowding (akin to ‘overcrowding dispersal’ in our model), provides some relevant background, these studies primarily focus on segregation phenomena. In contrast, our work examines aggregation scenarios where both populations interact within the same space. Our model introduces distinct dynamics for each population: transport for ρ_1 and granular dynamics for ρ_2 . Future work will investigate scenarios where both populations exhibit both transport and congestion behaviors. In the following section, we present the main results for the transport equation of ρ_1 , considering a bounded $W^{1,1}$ -velocity field V with bounded divergence.

Section 3 introduces a solution concept for the evolution problem (1) and establishes its existence using an implicit time discretization scheme within the framework of the 1–Wasserstein distance, W_1 , and the Kantorovich potential. This approach treats problem (1) in the flavor of a W_1 -gradient flow in the dual space of Lip_1 .

Section 4 outlines the numerical algorithm used in this study. Adapting the prediction-correction approach from [21], we first transport ρ_1 according to the transport equation (1). Subsequently, an implicit time discretization scheme is applied for the dynamics described in (1). The discrete dynamics for ρ_2 are then determined by a projection operator onto the set of admissible densities, ensuring $0 \leq \rho_1 + \rho_2 \leq 1$, which can be efficiently implemented using a minimal flow approach.

Finally, Section 6 presents a series of numerical simulations to illustrate the behavior of the model.

2. Transport flow in population ρ_1

2.1. Reminder on linear transport equation in a bounded domain. In the context of directed crowd movement, where individuals follow a predefined path towards

a specific destination, the velocity vector field V plays a crucial role. To accurately model this behavior, V is typically specified with a prescribed normal flux on the boundary. This ensures that the crowd movement aligns with the desired dynamics at the domain's edges.

We consider the transport equation

$$(2.1) \quad \begin{cases} \frac{\partial u}{\partial t} + \nabla \cdot (u V) = 0 & \text{in } Q \\ u(0) = u_0 & \text{in } \Omega, \end{cases}$$

where V is assumed to satisfy

$$(T1) \quad V \in L^1(0, T; W^{1,1}(\Omega)^N) \cap L^\infty(Q)^N$$

$$(T2) \quad \nabla \cdot V \in L^\infty(Q).$$

Under the previous assumptions, $V \cdot \nu \in L^\infty((0, T) \times \partial\Omega)$, where ν is the outward unit normal vector to the boundary $\partial\Omega$, is well defined. The behavior of the vector field V significantly influences population dynamics. In a closed area, where the population is confined, $V \cdot \nu = 0$ on the boundary $\partial\Omega$, signifying no population flux across the domain's edges. In an open domain, the sign of $V \cdot \nu$ determines the direction of population flow: $V \cdot \nu \geq 0$ allows for population outflow, while $V \cdot \nu \leq 0$ indicates population inflow. More complex scenarios arise when the sign of $V \cdot \nu$ changes along the boundary. For instance, $V \cdot \nu$ may be negative on some parts of the boundary, allowing inflow, and positive on others, enabling outflow, resulting in a dynamic where population enters and exits the domain through different sections of its boundary. This variability in the normal trace of V significantly influences the overall population dynamics within the domain.

Following [17, 19], to incorporate the boundary condition for (2.1), we define the inflow boundary as :

$$\Sigma^- := \left\{ (t, x) \in (0, T) \times \partial\Omega : V \cdot \nu < 0 \right\},$$

and consider the following evolution problem

$$(2.2) \quad \begin{cases} \frac{\partial u}{\partial t} + \nabla \cdot (u V) = 0 & \text{in } Q \\ u = 0 & \text{on } \Sigma^- \\ u(0) = u_0 & \text{in } \Omega. \end{cases}$$

THEOREM 2.1. *Assume V satisfies the assumption (T1) and (T2), and $u_0 \in L^\infty(\Omega)$, Then, the problem (2.1) has a unique weak solution u in the sense that : $u \in L^\infty(Q)$, $(u V) \cdot \nu \in L^\infty(\Sigma)$, $(u V) \cdot \nu = 0$, \mathcal{H}^{N-1} -a.e. on Σ^- , and*

$$\frac{d}{dt} \int_{\Omega} u \xi \, dx - \int_{\Omega} u V \cdot \xi \, dx = 0, \text{ in } \mathcal{D}([0, T]),$$

for any $\xi \in \mathcal{C}_c^\infty(\Omega)$. In particular, $(u V) \cdot \nu$ is uniquely well defined, and we have

$$(2.3) \quad \frac{d}{dt} \int_{\Omega} u \xi - \int_{\Omega} u V \cdot \nabla \xi = \int_{\Omega} f \xi - \int_{\partial\Omega} \xi u V \cdot \nu \, d\mathcal{H}^{N-1}, \text{ in } \mathcal{D}([0, T]).$$

If moreover, V satisfies

$$(2.4) \quad \nabla \cdot V \geq 0 \quad \text{a.e. in } Q.$$

and $0 \leq u_0$, then

$$0 \leq u(t) \leq \|u_0\|_\infty, \quad \text{a.e. in } Q.$$

PROOF. The results of this theorem are more or less well known by now. For the proof we refer the reader to the papers [17, 19] and also [2, 3, 5]. \square

REMARK 1. *Beyond boundary conditions, the divergence of the velocity field, $\nabla \cdot V$, plays a crucial role in population dynamics, particularly concerning congestion phenomena. Expansive velocity fields, characterized by $\nabla \cdot V \geq 0$, tend to prevent excessive population densities, while compressive velocity fields, where $\nabla \cdot V < 0$ can potentially lead to congestion and overcrowding.*

REMARK 2. *Taking $\xi \equiv 1$ in the formulation (2.1), we obtain the following mass conservation property*

$$\frac{d}{dt} \int_{\Omega} u \, dx = - \int_{\partial\Omega} \underbrace{u V \cdot \nu}_{\geq 0} \, d\mathcal{H}^{N-1}, \quad \text{in } \mathcal{D}([0, T]).$$

COROLLARY 2.1. *Under the assumptions of Theorem 2.1, if moreover*

$$(2.5) \quad V \cdot \nu \geq 0, \quad \mathcal{H}^{N-1} - \text{ a.e. on } \Sigma,$$

then, for any $u_0 \in L^\infty(\Omega)$, the problem

$$\begin{cases} \frac{\partial u}{\partial t} + \nabla \cdot (u V) = 0 & \text{in } Q \\ u(0) = u_0 & \text{in } \Omega, \end{cases}$$

has a unique weak solution u in the sense that : $u \in L^\infty(Q)$ and

$$\frac{d}{dt} \int_{\Omega} u \xi \, dx - \int_{\Omega} u V \cdot \xi \, dx = 0, \quad \text{in } \mathcal{D}([0, T]),$$

for any $\xi \in C_c^\infty(\Omega)$. In particular, $(u V) \cdot \nu \in L^\infty(\Sigma)$ is uniquely well defined.

PROOF. This is a consequence of Theorem 2.1 and the fact that, under the assumption (2.1), $\Sigma^- = \emptyset$. \square

2.2. Application to directed crowd motion for population ρ_1 . In this paper, we focus on admissible scenarios where the vector field V is such that the dynamics of population ρ_1 do not lead to congestion in the absence of population ρ_2 . So, we assume that V is a given vector field satisfying the assumptions (T1), (T2) and moreover (2.1). Then, let us consider $0 \leq \rho_{01} \leq 1$ representing the given initial density of population ρ_1 . Below, we present the key theoretical results which follow directly from the previous section. Notice that the assumptions on V we are dealing with are such the population is not concerned with the congestion ; i.e. $0 \leq \rho_1 \leq 1$ a.e. in Q . However, the evolution of ρ_1

will inevitably compel population ρ_2 to react in order to avoid the global congestion (the phenomenon concerning ρ_2 is treated in Section 3).

No population flux in a closed area: here we assume that no population exchange across certain sections of the boundary, represented by zero normal flux, effectively acting as walls. In this case the normal trace of V is such that

$$V \cdot \nu = 0, \quad \text{on } \Sigma.$$

Then, the evolution problem

$$\begin{cases} \frac{\partial \rho_1}{\partial t} + \nabla \cdot (\rho_1 V) = 0 & \text{in } Q \\ \rho_1(0) = \rho_{01} & \text{in } \Omega, \end{cases}$$

has a unique solution ρ_1 , which satisfies :

- $\rho_1 \in L^\infty(Q)$
- $0 \leq \rho_1 \leq 1$, a.e. in Q
- $(\rho_1 V) \cdot \nu = 0$, \mathcal{H}^{n-1} -a.e. on Σ
- for any $\xi \in \mathcal{C}^\infty(\bar{\Omega})$,

$$\frac{d}{dt} \int_{\Omega} \rho_1 \xi \, dx - \int_{\Omega} \rho_1 V \cdot \xi \, dx = 0, \quad \text{in } \mathcal{D}([0, T]).$$

- for a.e. $t \in (0, T)$, we have

$$\int_{\Omega} \rho_1(t, x) \, dx = \int_{\Omega} \rho_{01}(x) \, dx.$$

Population outflow in an open area: here we assume that we have an outflow of population, modeled by an outward normal flux at exit points. In this case

$$V \cdot \nu \geq 0, \quad \text{on } \Sigma.$$

Then, the evolution problem

$$\begin{cases} \frac{\partial \rho_1}{\partial t} + \nabla \cdot (\rho_1 V) = 0 & \text{in } Q \\ \rho_1(0) = \rho_{01} & \text{in } \Omega, \end{cases}$$

has a unique solution ρ_1 , which satisfies :

- $\rho_1 \in L^\infty(Q)$
- $0 \leq \rho_1 \leq 1$, a.e. in Q
- $0 \leq (\rho_1 V) \cdot \nu \in L^\infty(\Sigma)$,
- for any $\xi \in \mathcal{C}^\infty(\bar{\Omega})$,

$$\frac{d}{dt} \int_{\Omega} \rho_1 \xi \, dx - \int_{\Omega} \rho_1 V \cdot \xi \, dx = - \int_{\partial\Omega} (\rho_1 V) \cdot \nu \xi \, d\mathcal{H}^{n-1}, \quad \text{in } \mathcal{D}([0, T]).$$

- for a.e. $t \in (0, T)$, we have

$$\int_{\Omega} \rho_1(t, x) dx = \int_{\Omega} \rho_{01}(x) dx - \int_0^t \int_{\partial\Omega} (\rho_1 V) \cdot \nu d\mathcal{H}^{n-1}.$$

Mixed inflow-outflow population in input-output area: In this case, we assume that there exists a non-negligible subset $\Sigma^- \subset (0, T) \times \partial\Omega$, such that for a.e. $t \in (0, T)$,

$$V \cdot \nu < 0, \quad \text{on } \Sigma^+.$$

The evolution problem

$$\begin{cases} \frac{\partial \rho_1}{\partial t} + \nabla \cdot (\rho_1 V) = 0 & \text{in } Q \\ \rho_1 = 0 & \text{on } \Sigma^- \\ \rho_1(0) = \rho_{01} & \text{in } \Omega, \end{cases}$$

has a unique solution ρ_1 , which satisfies :

- $\rho_1 \in L^\infty(Q)$
- $0 \leq \rho_1 \leq 1$, a.e. in Q
- $0 \leq (\rho_1 V) \cdot \nu \in L^\infty(\Sigma)$,
- $\rho_1 V \cdot \nu = 0$ \mathcal{H}^{n-1} -a.e. on Σ^-
- for any $\xi \in C^\infty(\bar{\Omega})$,

$$\frac{d}{dt} \int_{\Omega} \rho_1 \xi dx - \int_{\Omega} \rho_1 V \cdot \xi dx = - \int_{\partial\Omega} (\rho_1 V) \cdot \nu \xi d\mathcal{H}^{n-1}, \text{ in } \mathcal{D}([0, T]).$$

- for a.e. $t \in (0, T)$, we have

$$\int_{\Omega} \rho_1(t, x) dx = \int_{\Omega} \rho_{01}(x) dx - \int_0^t \int_{\partial\Omega} (\rho_1 V) \cdot \nu d\mathcal{H}^{n-1}.$$

REMARK 3. *Despite restricting our theoretical analysis to the assumptions of Theorem 1, the algorithm and numerical computations remain effective in several broader scenarios:*

- (1) *Compressive vector fields with small initial data: our approach can be extended to compressive vector fields $\nabla \cdot V < 0$ coupled with small initial data ρ_{01} .*
- (2) *Non-local potential with Gaussian kernel: The velocity field V can be determined by a non-local potential, $V = -\nabla(\rho_1 \star K_\sigma)$, where K_σ is a Gaussian kernel. This captures the influence of neighboring individuals on population movement and ensures a repulsive effect, preventing overcrowding. While primarily capturing repulsive behaviors, this framework can be adapted to study aggregative phenomena.*
- (3) *Diffusion-based potential: Alternatively, we can employ the Green's function of the Laplacian as the kernel, effectively solving a diffusion equation at each step to determine the potential for V . This diffusion-based approach provides a more nuanced representation of the influence of neighboring individuals on population movement.*

3. Congestion management theory

3.1. Developing a congestion management model. As discussed in the introduction, spatial constraints can lead to congestion when the directed movement of the first population interacts with the second population of density ρ_2 . Specifically, the total density, $\rho_1 + \rho_2$, may exceed the maximum permissible density, $\rho_{max} = 1$. While population ρ_1 maintains its singular focus on its objective, following the prescribed velocity field V , and disregards any global congestion, we introduce a 'decongestion' mechanism for the initially static population ρ_2 to prevent congestion arising from their interaction with ρ_1 . We propose a dynamic model for this scenario, inspired by the behavior of grains of sand settling into a stable heap. The first population can be likened to a continuous influx of sand that exerts pressure on the existing structure, while the second population represents the existing sand grains that are effectively rearranged to accommodate these new additions.

To this aim, we consider the following evolution problem:

$$(3.1) \quad \frac{d\rho_2}{dt} + \partial \mathbb{I}_{\text{Lip}_1}(p) \ni 0, \quad \text{in } (0, T)$$

where p is the Lagrange multiplier associated with the constraint $\rho_1 + \rho_2 \leq 1$; i.e.

$$(3.2) \quad p \geq 0, \quad 0 \leq \rho_2 \leq 1 - \rho_1, \quad p(1 - (\rho_1 + \rho_2)) = 0, \quad \text{in } Q.$$

Here $\partial \mathbb{I}_{\text{Lip}_1}(p)$ denotes the sub-differential of the indicator function of Lip_1 , the set of 1-Lipschitz functions on Ω , defined as:

$$\mathbb{I}_{\text{Lip}_1}(p) = \begin{cases} 0 & \text{if } p \in \text{Lip}_1 \\ +\infty & \text{otherwise.} \end{cases}$$

The precise definition of $\partial \mathbb{I}_{\text{Lip}_1}$ using the duality pairing will be provided in Section 3.2 (see (3.2)). Remember that (cf. [1, 20, 29, 30]), the evolution problem (3.1) can be reformulated in terms of PDE as:

$$(3.3) \quad \left. \begin{cases} \frac{\partial \rho_2}{\partial t} - \nabla \cdot (m \nabla p) = 0 \\ m \geq 0, |\nabla p| \leq 1, m(1 - |\nabla p|) = 0, \end{cases} \right\} \quad \text{in } Q,$$

subject to (3.1) and Neumann boundary condition:

$$(3.4) \quad m \nabla p \cdot \nu = 0 \quad \text{on } \Sigma.$$

Indeed, this formulation is closely connected to the observation that, employing a test function of the form $p - \xi$, where $\xi \in \text{Lip}_1$, in equation (3.1), we formally obtain:

$$\int_{\Omega} \partial_t \rho_2 (p - \xi) = - \int_{\Omega} m \nabla p \cdot \nabla (p - \xi) = \int_{\Omega} m(1 - \nabla p \cdot \nabla \xi) \leq 0,$$

which is equivalent to

$$-\partial_t \rho_2 \in \partial \mathbb{I}_{\text{Lip}_1}(p).$$

However, as is typical for this equivalence, m is generally a Radon measure. This requires the use of the tangential gradient for the gradient of p , a specialized approach (see [8] for further details). To circumvent this complexity, we focus on the variational formulation

(3.1), drawing inspiration from studies such as [1, 20, 29, 30] that address similar problems in slightly different contexts.

The function ρ_1 in (3.1) and (3.1) is given by the solution of the transport equation from the previous section. Specifically, it is assumed that $\rho_1 \in L^\infty(Q)$, $0 \leq \rho_1 \leq 1$ a.e. in Q , and satisfies:

$$(3.5) \quad \frac{d}{dt} \int_{\Omega} \rho_1 \xi \, dx = \int_{\Omega} \rho_1 V \cdot \xi \, dx, \text{ in } \mathcal{D}([0, T]).$$

for any $\xi \in \mathcal{C}_c^\infty(\Omega)$. Here $V \in L^\infty(Q)^N \cap L^1(0, T, W^{1,1}(\Omega)^N)$ and $0 \leq \nabla \cdot V \in L^\infty(Q)$.

As previously mentioned, the variational approach will play a crucial role in our characterization of the solutions to (3.1). However, before proceeding further with the formulation, it's important to note that the key term $\int_{\Omega} \partial_t \rho_2 (p - \xi)$ in the variational formulation associated with (3.1) necessitates increased regularity assumptions on either ρ_1 , ρ_2 or p , which are not generally expected to hold. Indeed, using (3.1), we formally see that

$$(3.6) \quad \begin{aligned} \int_{\Omega} \partial_t \rho_2 (p - \xi) &= \int_{\Omega} \partial_t (1 - \rho_1) p - \int_{\Omega} \partial_t \rho_2 \xi \\ &= - \int_{\Omega} \partial_t \rho_1 p - \int_{\Omega} \partial_t \rho_2 \xi \\ &= - \int_{\Omega} \partial_t \rho_1 p - \frac{d}{dt} \int_{\Omega} \rho_2 \xi. \end{aligned}$$

Contrary to the findings reported in the aforementioned studies ([31, 1]) where ρ_1 was essentially zero, the non-zero nature of ρ_1 in this study renders the application of the same approach employed in [31, 1] ineffective.

To circumvent this issue, we propose to incorporate the transport equation (2.1) into (3.1), achieving the nonlinear dynamic for the total density $\rho := \rho_1 + \rho_2$:

$$\frac{d}{dt} \rho + \partial \mathbb{H}_{\text{Lip}_1}(p) \ni f$$

where $f := -\nabla \cdot (\rho_1 V)$. Since ρ_1 is a solution of the transport equation (2.1), $f = -\nabla \cdot (\rho_1 V)$, should to be understood in distributional sense :

$$(3.7) \quad \begin{aligned} \langle f(t), \xi \rangle &= \int_{\Omega} \rho_1(t, x) V(t, x) \cdot \nabla \xi(x) \, dx \\ &- \int_{\partial \Omega} (\rho_1(t, x) V(t, x)) \cdot \nu(x) \xi(x) \, d\mathcal{H}^{n-1}(x), \end{aligned}$$

for any $\xi \in \mathcal{C}^\infty(\bar{\Omega})$, which is well defined. The formulation (3.1) can also be interpreted within the framework of the duality bracket between Lip , the space of 1-Lipschitz functions, and Lip' , its topological dual space, which will be introduced later.

In the preceding section, the density was characterized by ρ_1 . In this section, the focus will be on solving the evolution problem (3.1) and (3.1). Following the same line of reasoning as in the formal computation (3.1), we observe that:

$$\int_{\Omega} \partial_t \rho (p - \xi) = -\frac{d}{dt} \int_{\Omega} \rho \xi.$$

Combining this observation with the definition of $\partial \mathbb{I}_{\text{Lip}_1}$, we arrive at the following variational formulation for the total density :

$$-\frac{d}{dt} \int_{\Omega} \rho \xi \leq \langle f, p - \xi \rangle, \quad \text{in } \mathcal{D}'([0, T]).$$

That is

$$(3.8) \quad -\frac{d}{dt} \int_{\Omega} \rho \xi - \int_{\Omega} \rho_1 V \cdot \nabla (p - \xi) dx \leq - \int_{\partial \Omega} (\rho_1 V) \cdot \nu (p - \xi) d\mathcal{H}^{n-1}, \quad \text{in } \mathcal{D}'([0, T]),$$

for any $\xi \in \text{Lip}_1$.

Finlay, the study of the management of the congested crossing pedestrian traffic flow follows by first solving the transport equation as in the previous section, and then solving the evolution problem (3.1) combined with the state equation (3.1) through the variational formulation (3.1).

3.2. Theoretical study. Thanks to the last section, we now focus on the theoretical study of the evolution problem.

$$(3.9) \quad \begin{cases} \frac{\partial \rho}{\partial t} + \partial \mathbb{I}_{\text{Lip}_1}(p) = f \\ 0 \leq p, 0 \leq \rho \leq 1, p(1 - \rho) = 0, \\ \rho(0) = \rho_{01} + \rho_{02}, \end{cases}$$

where $f = -\nabla \cdot (\rho_1 V)$ is given by (3.1) and ρ_1 satisfy (3.1) with $\rho_2(0) = \rho_{02}$.

Thanks to the discussion above, the notion of solution we have in mind is given as follows :

DEFINITION 3.1. *A function ρ_2 is said to be a weak solution of (3.2), if $0 \leq \rho_2 \in L^\infty(Q)$, $0 \leq \rho := \rho_1 + \rho_2 \leq 1$ a.e. in Q and, there exists $0 \leq p \in L^\infty(Q)$, s.t. $p(t) \in \text{Lip}_1$, a.e. $t \in (0, T)$, $p(1 - \rho) = 0$, a.e. in Q , and*

$$(3.10) \quad -\frac{d}{dt} \int_{\Omega} (\rho_1 + \rho_2) \xi \leq \langle f, p - \xi \rangle, \quad \text{in } \mathcal{D}'([0, T]),$$

for any $\xi \in \text{Lip}_1$, $\rho_2(0) = \rho_{02}$.

REMARK 4. *By definition of f , equation (3.1) can be rewritten as*

$$-\frac{d}{dt} \int_{\Omega} (\rho_1 + \rho_2) \xi \leq \int_{\Omega} \rho_1 V \cdot \nabla (p - \xi) dx - \int_{\partial \Omega} (\rho_1 V) \cdot \nu (p - \xi) d\mathcal{H}^{n-1}, \quad \text{in } \mathcal{D}'([0, T]),$$

for any $\xi \in \text{Lip}_1$. This, in turn, is equivalent, by virtue of (3.1), to

$$-\frac{d}{dt} \int_{\Omega} \rho_2 \xi \leq \int_{\Omega} \rho_1 V \cdot \nabla p \, dx - \int_{\partial\Omega} (\rho_1 V) \cdot \nu p \, d\mathcal{H}^{n-1}, \quad \text{in } \mathcal{D}'([0, T]),$$

We suggest studying problem (3.2) using 1-Wasserstein distance, W_1 , and the Kantorovich potential. To do this, we will use the following notations and tools related to W_1 (a complete overview of the theory in may be found in the book [36]).

- $\text{Lip} := W^{1,\infty}(\Omega)$ the set of Lipschitz functions on Ω ,
- Lip_1 the set of 1-Lipschitz functions on Ω .
- $\text{Lip}'_0 := \{h \in \text{Lip}' : \langle h, 1 \rangle = 0\}$, where Lip' is the dual (topological) space of Lip and $\langle \cdot, \cdot \rangle$ denotes the duality pairing between Lip' and Lip .
- For any $h \in \text{Lip}'_0$, we denote by W_1 the dual semi-norm of h :

$$W_1(h) := \sup_{\theta \in \text{Lip}_1} \langle h, \theta \rangle.$$

When h is signed measure of the form $h = h^+ - h^-$, with h^{\pm} probability measures on $\bar{\Omega}$, $W_1(h)$ is the 1-Wasserstein distance between h^+ and h^- (see [36]).

- For a general $h \in \text{Lip}'_0$, $W_1(h)$ may be infinite. To ensure $W_1(h) < \infty$, one needs to restrict h to a space X' , where $\text{Lip} \subset X$ is such that the embedding of Lip into X is compact. A function $\theta \in \text{Lip}_1$ for which $W_1(h) = \langle h, \theta \rangle$ is called a Kantorovich potential of h . We restrict our attention to non-negative potentials, as it is always possible to find at least one such potential whenever the existence of a potential is guaranteed. We denote by $\mathcal{K}(h)$ the set of all Kantorovich potentials of h , that is:

$$\mathcal{K}(h) := \{0 \leq \theta \in \text{Lip}_1 : \langle h, \theta \rangle \geq \langle h, \psi \rangle, \forall \psi \in \text{Lip}_1\}.$$

In particular, this enables to define $\partial \mathcal{I}_{\text{Lip}_1}(p)$ in terms of Kantorovich potential as follows :

$$(3.11) \quad h \in \partial \mathcal{I}_{\text{Lip}_1}(p) \iff p \in \text{Lip}_1, h \in \text{Lip}'_0 \text{ and } p \in \mathcal{K}(h).$$

- Fenchel-Rockafellar duality theorem gives the following dual formula for $W_1(h)$:

$$(3.12) \quad W_1(h) = \inf_{\sigma \in (L^\infty(\Omega)')^N} \left\{ \|\sigma\|_{(L^\infty(\Omega)')^N} : \langle \sigma, \nabla \xi \rangle \, dx = \langle h, \xi \rangle, \forall \xi \in \text{Lip} \right\}.$$

Moreover, one can prove that for any $g \in \text{Lip}'_0$, (3.2) admits solutions (in $(L^\infty(\Omega)')^N$ and not in L^1 in general), such solutions are called optimal flows. A Kantorovich potential $\theta \in \mathcal{K}(h)$ is related to an optimal flow σ in (3.2) by the extremality relation

$$\langle \sigma, \nabla \theta \rangle_{(L^\infty(\Omega)')^N, L^\infty(\Omega)^N} = \|\sigma\|_{(L^\infty(\Omega)')^N} \text{ with } \|\nabla \theta\|_{L^\infty} \leq 1$$

which, very informally, means that σ is concentrated on the set where $|\nabla \theta|$ equals 1 and is collinear to $\nabla \theta$. If $\sigma \in L^1$, then previous relation reveals that $\sigma = m \nabla \theta$ with $m \geq 0$ and satisfies the complementary condition $m(1 - |\nabla \theta|) = 0$. This finding formally supports the formulation of equation (3.2) based on PDE (3.1).

Furthermore, the flux σ exhibits a tangential alignment with the boundary $\partial\Omega$ in a weak sense.

- For an arbitrary $h \in \text{Lip}'$ (not necessarily balanced), we can define

$$\widetilde{W}_1(h) := W_1\left(\underbrace{h - \frac{1}{|\Omega|}\langle h \rangle}_{=: \hat{h}}\right) + \frac{1}{|\Omega|}|\langle h \rangle|$$

and observe that \widetilde{W}_1 is equivalent to the usual norm of Lip' . When there is non confusing, we'll use again the notation $W_1(h)$ instead of $\widetilde{W}_1(h)$ even if $h \in \text{Lip}' \setminus \text{Lip}'_0$.

Given that $f(t)$, defined by (3.1) for a.e. $t \in (0, T)$, belongs to Lip' , for any $z \in \text{Lip}_1$, we have

$$\begin{aligned} \langle f(t), z \rangle &= \langle \hat{f}(t), z \rangle + \langle f(t) \rangle \oint_{\Omega} z \\ (3.13) \qquad &\leq W_1(\hat{f}(t)) + \langle f(t) \rangle \oint_{\Omega} z. \end{aligned}$$

Furthermore, both $\langle f(t) \rangle$ and $W_1(\hat{f}(t))$ are well defined and belong to the space $L^\infty(0, T)$. Indeed, for a.e. $t \in (0, T)$, we have

$$\langle f(t) \rangle = - \int_{\partial\Omega} (\rho_1 V) \cdot \nu \, d\mathcal{H}^{n-1}, \quad \text{for a.e. } t \in (0, T),$$

and, moreover we see that

$$\begin{aligned} W_1(\hat{f}(t)) &= \max_{\theta \in \text{Lip}_1} \langle f(t), \theta \rangle - \oint_{\Omega} \theta \\ &= \max_{\theta \in \text{Lip}_1} \left\{ \int_{\Omega} \rho_1(t) V(t) \cdot \nabla \theta \, dx - \int_{\partial\Omega} (\rho_1 V) \cdot \nu (\theta - \oint_{\Omega} \theta) \, d\mathcal{H}^{n-1} \right\} \\ &\leq C(\Omega, N) (\|V(t)\|_1 + \|(\rho_1 V) \cdot \nu\|_{L^1(\partial\Omega)}). \end{aligned}$$

Now, considering the previous observations, it is natural to interpret the evolution problem (3.2) as the inclusion

$$(3.14) \quad p(t) \in \mathcal{K}(f(t) - \partial_t \rho(t)), \quad 0 \leq \rho(t) \leq 1, \quad 0 \leq p(t), \quad p(t)(1 - \rho(t)) = 0,$$

for any $t \in (0, T)$. In particular, one sees that this formulation inherently imposes a conservation of mass, represented by

$$\langle f(t) - \partial_t \rho(t) \rangle = 0, \quad \text{for any } t \in [0, T],$$

which aligns with the boundary condition in (3.1) and the weak formulation (3.1). Moreover, thanks to the definition of f , (3.1) implies that

$$\frac{d}{dt} \int_{\Omega} \rho(t) \, dx = \langle f(t) \rangle = - \int_{\partial\Omega} (\rho_1(t) V(t)) \cdot \nu \, d\mathcal{H}^{n-1}, \quad \text{for a.e. } t \in (0, T),$$

which implies in turns

$$\mathcal{M}(t) := \int_{\Omega} \rho(t) dx = \int_{\Omega} \rho_0 dx + \int_0^t \langle f(t) \rangle dt.$$

Since $0 \leq \rho \leq 1$ a.e. in Q , this property implies a necessary condition for the existence of a solution to the problem (3.2) :

$$0 \leq \mathcal{M}(t) \leq |\Omega|, \quad \text{for a.e. } t \in (0, T).$$

With all this in mind, we can now state the main result of this section.

THEOREM 3.2. *Let $0 \leq \rho_{02} \in L^\infty(\Omega)$, be such that $0 \leq \rho_{01} + \rho_{02} \leq 1$ a.e. in Ω , and satisfying moreover*

$$(3.15) \quad \sup_{t \in [0, T)} \mathcal{M}(t) =: \overline{\mathcal{M}} < |\Omega|, \quad \text{for a.e. } t \in (0, T).$$

Then, the problem (3.2) has a weak solution ρ_2 in the sense of Definition 3.1. Moreover, we have

$$(3.16) \quad \int_{\Omega} (\rho_1(t) + \rho_2(t)) dx = \mathcal{M}(t), \quad \text{a.e. } t \in [0, T),$$

and

$$(3.17) \quad \frac{d}{dt} \int_{\Omega} \rho_2(t) dx = 0.$$

REMARK 5. (1) *Since $0 \leq \rho_{02} \leq 1$, instead of working with condition (3.2) in all the time interval $(0, T)$, one can replace T , by T_a given by*

$$T_a := \sup \{t \in [0, T) : 0 \leq \mathcal{M}(s) < |\Omega|, \quad \text{for a.e. } s \in (0, t)\}.$$

Yet, one needs to assume that $T_a > 0$.

(2) *By definition fo f , one sees that*

$$\begin{aligned} \mathcal{M}(t) &= \int_{\Omega} \rho_0 dx - \int_0^t \int_{\partial\Omega} (\rho_1(t) V(t)) \cdot \nu d\mathcal{H}^{n-1}, \quad \text{for a.e. } t \in (0, T) \\ &= \int_{\Omega} \rho_0 dx - \int_{\Omega} \rho_{01} dx + \int_{\Omega} \rho_1(t) dx, \quad \text{for a.e. } t \in (0, T) \\ &= \int_{\Omega} \rho_{02} dx + \int_{\Omega} \rho_1(t) dx, \quad \text{for a.e. } t \in (0, T) \\ &= \int_{\Omega} (\rho_1(t) + \rho_2(t)) dx, \quad \text{for a.e. } t \in (0, T). \end{aligned}$$

Condition (3.2) ensures that the combined density of both populations ρ_1 and ρ_2 remains strictly below 1 at any given time. This means there is always a free space within the domain, allowing for the population to undergo its correction dynamics.

With the equivalence (3.2) in consideration, we propose solving the evolution problem (3.2) using an Euler implicit scheme. For a given time-step $\tau > 0$, the implicit time discretization associated with (3.2) is given by:

$$(3.18) \quad p_{k+1}^\tau \in \mathcal{K}\left(f_k^\tau - \frac{\rho_{k+1} + \rho_k}{\tau}\right), \quad 0 \leq \rho_{k+1}^\tau \leq 1, \quad 0 \leq p_{k+1}^\tau, \quad p_{k+1}^\tau(1 - \rho_{k+1}) = 0,$$

for $k = 0, \dots, m-1$, where $m := [T/\tau]$ and f_k^τ is given by

$$f_k^\tau = \frac{1}{\tau} \int_{k\tau}^{(k+1)\tau} f(t) dt, \quad \text{for any } k = 0, \dots, m-1.$$

Here, we know the value of ρ_k^τ , but we need to find the values of p_{k+1}^τ and ρ_{k+1}^τ . Thanks to the definition of \mathcal{K} , we also have

$$(3.19) \quad p_{k+1}^\tau \in \mathcal{K}\left(\rho_k^\tau + \tau f_k^\tau - \rho_{k+1}\right), \quad 0 \leq \rho_{k+1}^\tau \leq 1, \quad 0 \leq p_{k+1}^\tau, \quad p_{k+1}^\tau(1 - \rho_{k+1}^\tau) = 0.$$

That is $p_{k+1}^\tau \in \text{Lip}_1$ and

$$(3.20) \quad \langle \rho_k^\tau + \tau f_k^\tau - \rho_{k+1}, p_{k+1}^\tau - \psi \rangle \geq 0, \quad \forall \psi \in \text{Lip}_1,$$

with

$$0 \leq \rho_{k+1}^\tau \leq 1, \quad 0 \leq p_{k+1}^\tau, \quad p_{k+1}^\tau(1 - \rho_{k+1}^\tau) = 0.$$

The following lemma provides a means to determine ρ_{k+1} and p_{k+1} , and to implement the Euler implicit scheme (3.2).

LEMMA 3.1. *Given a time step $\tau > 0$, for any $k = 1, \dots, m$, the sequences ρ_k^τ and p_k^τ in (3.2) are well defined inductively by*

$$(3.21) \quad \begin{aligned} \rho_k^\tau \in \operatorname{argmin}_u \left\{ W_1(\rho_{k-1}^\tau + \tau f_{k-1}^\tau - u) : \langle \rho_{k-1}^\tau + \tau f_{k-1}^\tau - u \rangle = 0, \right. \\ \left. u \in L^\infty(\Omega), 0 \leq u \leq 1 \right\}, \end{aligned}$$

and

$$(3.22) \quad p_k^\tau \in \operatorname{argmax}_\theta \left\{ \langle \rho_{k-1}^\tau + \tau f_{k-1}^\tau, \theta \rangle - \int \theta : 0 \leq \theta \in \text{Lip}_1 \right\}$$

by setting $\rho_0^\tau = \rho_{01}$. Moreover, we have

$$W_1(\rho_{k-1}^\tau + \tau f_{k-1}^\tau - \rho_k^\tau) = \langle \rho_{k-1}^\tau + \tau f_{k-1}^\tau, p_k^\tau \rangle - \int p_k^\tau$$

PROOF. Existence for (3.1) follows from the fact that W_1 is lsc for the weak L^p -topology, for any $1 \leq p \leq \infty$. As to (3.1), it follows by duality. Indeed, using the definition of f , we have

$$W_1(\rho_{k-1}^\tau + \tau f_{k-1}^\tau - u) = \max_{0 \leq \theta \in \text{Lip}_1} \langle \rho_{k-1}^\tau + \tau f_{k-1}^\tau - u, \theta \rangle,$$

so that

$$\begin{aligned} I_{k-1} &:= \min_{u \in L^\infty(\Omega)} \left\{ W_1(\rho_{k-1}^\tau + \tau f_{k-1}^\tau - u) : \langle \rho_{k-1}^\tau + \tau f_{k-1}^\tau - u \rangle = 0, 0 \leq u \leq 1 \right\} \\ &= \min_{u \in L^\infty(\Omega)} \max_{0 \leq \theta \in \text{Lip}_1} \left\{ \langle \rho_{k-1}^\tau + \tau f_{k-1}^\tau - u, \theta \rangle : \langle \rho_{k-1}^\tau + \tau f_{k-1}^\tau - u \rangle = 0, 0 \leq u \leq 1 \right\}. \end{aligned}$$

We can use the Von Neumann-Fan minimax theorem (see for instance [10]), to prove this, just like we did for the proof of Proposition 4.5 in the work [21], we get

$$\begin{aligned} I_{k-1} &= \max_{0 \leq \theta \in \text{Lip}_1} \min_{u \in L^\infty(\Omega)} \left\{ \langle \rho_{k-1}^\tau + \tau f_{k-1}^\tau - u, \theta \rangle : \langle \rho_{k-1}^\tau + \tau f_{k-1}^\tau - u \rangle = 0, 0 \leq u \leq 1 \right\} \\ &= \max_{0 \leq \theta \in \text{Lip}_1} \left\{ \langle \rho_{k-1}^\tau + \tau f_{k-1}^\tau, \theta \rangle - \int \theta \right\}. \end{aligned}$$

Moreover, taking ρ_k and p_k given by (3.1) and (3.1), respectively, one sees the couple (ρ_k, p_k) solves the equation (3.2). \square

Clearly, the algorithm (3.2), for $k = 0, \dots, m-1$, follows the implicit Euler scheme à la Jordan-Kinderlehrer-Otto (cf. [32]) to construct weak solutions, but using W_1 instead of the more familiar 2-Wasserstein distance, W_2 , and incorporating the source explicitly in the scheme with 1-Wasserstein.

To prove the convergence of the implicit Euler scheme with the solution given in Theorem 3.2, we first establish some preliminary results. We define two curves corresponding to piecewise constant and linear interpolation:

$$\rho^\tau(t) := \rho_{k+1}^\tau \quad \text{and} \quad \tilde{\rho}^\tau(t) := \rho_k^\tau + \frac{t - k\tau}{\tau} (\rho_{k+1}^\tau - \rho_k^\tau), \quad \text{for any } t \in (k\tau, (k+1)\tau],$$

for $k = 0, \dots, m$. We also define the piecewise constant approximation of f :

$$f^\tau(t) := f_k^\tau, \quad t \in (k\tau, (k+1)\tau], \quad k = 0, \dots, m,$$

and the piecewise constant approximation

$$p^\tau(t) := p_{k+1}^\tau, \quad t \in (k\tau, (k+1)\tau].$$

Thanks to (3.2), we see that

$$\langle \rho_k^\tau \rangle = \mathcal{M}(k\tau) \leq \overline{\mathcal{M}}, \quad \text{for any } k = 0, \dots, m.$$

Indeed, by construction

$$\begin{aligned} (3.23) \quad \langle \rho_k^\tau \rangle &= \langle \rho_{k-1}^\tau + \tau f_{k-1}^\tau \rangle \\ &= \int_{\Omega} \rho_0(x) dx + \tau \sum_{i=0}^{k-1} \langle f_i^\tau \rangle \\ &= \int_{\Omega} \rho_0(x) dx + \int_0^{k\tau} \langle f(t) \rangle dt = \mathcal{M}(k\tau). \end{aligned}$$

The goal now is to get to the limit in (3.2), as $\tau \rightarrow 0$, this is the main objective of the sequence of the following lemmas.

LEMMA 3.2. p^τ is bounded in $L^\infty(0, T; \text{Lip}_1)$.

PROOF. By definition of p^τ , we know that

$$\|\nabla p^\tau\|_{L^\infty((0, T) \times \Omega)} \leq 1, \quad \text{a.e. in } Q.$$

This implies that, for any $t \in [0, T]$, $p^\tau(t) - \oint_\Omega p^\tau(t)$ is bounded in Lip_1 . On the other hand, using (3.2), we have

$$\langle \rho_{k+1}^\tau - \rho_k^\tau, p_{k+1}^\tau \rangle \leq \tau \langle f_k^\tau, p_{k+1}^\tau \rangle.$$

Combining this with (3.2), we get

$$\int_\Omega (\rho_{k+1}^\tau - \rho_k^\tau) p_{k+1}^\tau \leq \tau W_1(\widehat{f_k^\tau}) + \tau \langle f_k^\tau \rangle \oint_\Omega p_{k+1}^\tau.$$

Using the fact that $\rho_{k+1}^\tau p_{k+1}^\tau = p_{k+1}^\tau$, we get

$$\langle p_{k+1}^\tau \rangle \leq \tau W_1(\widehat{f_k^\tau}) + \tau \langle f_k^\tau \rangle \oint_\Omega p_{k+1}^\tau + \int_\Omega \rho_k^\tau p_{k+1}^\tau.$$

This implies that

$$\langle p_{k+1}^\tau \rangle \leq \tau W_1(\widehat{f_k^\tau}) + \underbrace{(\langle \rho_k^\tau \rangle + \tau \langle f_k^\tau \rangle)}_{\mathcal{M}((k+1)\tau)} \oint_\Omega p_{k+1}^\tau + \int_\Omega \rho_k^\tau (p_{k+1}^\tau - \oint_\Omega p_{k+1}^\tau),$$

and then

$$\oint_\Omega p_{k+1}^\tau (|\Omega| - \mathcal{M}((k+1)\tau)) \leq \tau W_1(\widehat{f_k^\tau}) + \int_\Omega \rho_k^\tau (p_{k+1}^\tau - \oint_\Omega p_{k+1}^\tau).$$

Remember that $\mathcal{M}((k+1)\tau) \leq \overline{\mathcal{M}} < |\Omega|$. So

$$\oint_\Omega p_{k+1}^\tau \leq \frac{\tau W_1(\widehat{f_k^\tau}) + \int_\Omega |p_{k+1}^\tau - \oint_\Omega p_{k+1}^\tau|}{|\Omega| - \overline{\mathcal{M}}},$$

and then

$$\oint_\Omega p^\tau(t) \leq \frac{\tau W_1(\widehat{f^\tau}(t)) + \int_\Omega |p^\tau(t) - \oint_\Omega p^\tau(t)|}{|\Omega| - \overline{\mathcal{M}}}, \quad \text{for any } t \in (k\tau, (k+1)\tau].$$

Using moreover, the fact that $p^\tau(t) - \oint_\Omega p^\tau(t) dx$ and $W_1(\widehat{f^\tau}(t))$ are bounded in $L^\infty(0, T)$, we deduce the result of the lemma. \square

LEMMA 3.3. *There exist a vanishing sequence of time steps, $\tau_n \rightarrow 0$ as $n \rightarrow \infty$, $0 \leq \rho \in L^\infty(Q)$ and $0 \leq p \in L^\infty(Q)$, such that $p(t) \in \text{Lip}_1$ for a.e. $t \in (0, T)$ and setting $\rho_n := \rho^{\tau_n}$, $\tilde{\rho}_n := \tilde{\rho}^{\tau_n}$ and $p_n := p^{\tau_n}$, we have :*

$$(3.24) \quad \rho_n \rightarrow \rho, \quad \text{in } L^\infty(Q) - \text{weak}^*,$$

$$(3.25) \quad \tilde{\rho}_n \rightarrow \rho, \quad \text{in } L^\infty(Q) - \text{weak}^*,$$

and

$$(3.26) \quad p_n \rightarrow p, \quad \text{in } L^q(0, T; W^{1,q}(\Omega)) - \text{weak}, \quad \forall q \in (1, +\infty).$$

Moreover, we have $0 \leq \rho \leq 1$ and $p(1 - \rho) = 0$ a.e. in Q .

PROOF. Clearly (3.3) follows by Lemma 3.2. We give here the main estimates concerning ρ^τ and $\tilde{\rho}^\tau$. Using $\rho_k^\tau + \frac{\tau}{|\Omega|} \langle f_k^\tau \rangle$ as a competitor to ρ_{k+1}^τ in (3.1), we see first :

$$\begin{aligned} W_1(\rho_{k+1}^\tau - (\rho_k^\tau + \tau f_k^\tau)) &\leq W_1(\tau \widehat{f_k^\tau}) \\ &\leq \int_{k\tau}^{(k+1)\tau} W_1(\widehat{f}(t)) dt \end{aligned}$$

Hence,

$$(3.27) \quad \sum_{k=0}^{m-1} W_1(\rho_{k+1}^\tau - \rho_k^\tau - \tau f_k^\tau) \leq \int_0^T W_1(\widehat{f}(t)) dt.$$

Next, by definition of $\tilde{\rho}^\tau$, we observe that,

$$\begin{aligned} \int_{k\tau}^{(k+1)\tau} W_1(\widehat{\partial_t \tilde{\rho}^\tau}(t)) &= \tau W_1(\widehat{\partial_t \tilde{\rho}^\tau}(t)) \\ &= W_1(\widehat{\rho_{k+1}^\tau - \rho_k^\tau}) \\ &\leq W_1(\rho_{k+1}^\tau - \rho_k^\tau - \tau f_k^\tau) + \tau W_1(\widehat{f_k^\tau}), \end{aligned}$$

so that

$$\int_0^T W_1(\widehat{\partial_t \tilde{\rho}^\tau}(t)) dt \leq \sum_{k=0}^{m-1} W_1(\rho_{k+1}^\tau - \rho_k^\tau - \tau f_k^\tau) + \int_0^T W_1(\widehat{f}(t)) dt.$$

Together with (3.2) and the fact that $\langle \partial_t \tilde{\rho}^\tau(t) \rangle = \langle f^\tau(t) \rangle$, for any $t \in [0, T]$, we deduce

$$(3.28) \quad \|\partial_t \tilde{\rho}^\tau\|_{L^1(0, T, (\text{Lip}', \widetilde{W}_1))} \leq C(\Omega) \int_0^T \widetilde{W}_1(f(t)) dt.$$

Combining this with the fact that $|\tilde{\rho}^\tau(t) - \rho^\tau| \leq \tau |\partial_t \tilde{\rho}^\tau|$, in $[k\tau, (k+1)\tau)$, we obtain

$$\|\rho^\tau - \tilde{\rho}^\tau\|_{L^1(0, T, (\text{Lip}', \widetilde{W}_1))} \leq C(\Omega) \tau \int_0^T \widetilde{W}_1(f(t)) dt.$$

Having in mind that ρ^τ and $\tilde{\rho}^\tau$ are bounded in $L^\infty(Q) - \text{weak}^*$, we conclude (3.3) and (3.3). To prove that $p(1 - \rho) = 0$ a.e. in Q , we employ first the theory of weak compensated compactness (cf. [5, 35]) with (3.2), (3.3) and (3.3) to deduce first that

$$p_n \tilde{\rho}_n \rightarrow p \rho, \quad \text{in } L^\infty(Q) - \text{weak}^*.$$

Then, clearly

$$(3.29) \quad p_n(1 - \tilde{\rho}_n) \rightarrow p(1 - \rho), \quad \text{in } L^\infty(Q) - \text{weak}^*.$$

On the other, using the fact that $p_n(1 - \rho_n) = 0$, a.e. Q , and (3.2), we see that

$$\begin{aligned}
0 \leq \int_0^T \int_{\Omega} p_n(1 - \tilde{\rho}_n) dt dx &= \int_0^T \int_{\Omega} p_n(\rho_n - \tilde{\rho}_n) dt dx \\
&\leq \tau_n \int_0^T \int_{\Omega} p_n \partial_t \tilde{\rho}_n dt dx \\
&\leq \tau_n \left\{ \int_0^T W_1(\widehat{\partial_t \tilde{\rho}_n(t)}) dt + \int_0^T \langle \partial_t \tilde{\rho}_n \rangle \oint_{\Omega} p_n dt \right\} \\
&\leq \tau_n \left\{ \int_0^T W_1(\widehat{f(t)}) dt + \int_0^T \langle f(t) \rangle \oint_{\Omega} p_n(t) dt \right\} \\
&\leq \tau_n C(\Omega, N) \quad \rightarrow 0, \quad \text{as } n \rightarrow \infty,
\end{aligned}$$

where we use, by Lemma 3.2, the fact that $\oint_{\Omega} p_n$ is bounded in $L^\infty(0, T)$. Then letting $n \rightarrow \infty$ and using (3.2), we deduce that $p(1 - \rho) = 0$ a.e. in Q . \square

PROOF OF THEOREM 3.2. Remember that

$$p_{k+1}^\tau \in \mathcal{K}(\rho_k^\tau + \tau f_k^\tau - \rho_{k+1}^\tau) = \mathcal{K}\left(f_k^\tau - \frac{\rho_{k+1}^\tau - \rho_k^\tau}{\tau}\right)$$

which can be rewritten as, for a.e. $t \in [0, T]$,

$$p^\tau(t) \in \mathcal{K}(f^\tau(t) - \partial_t \tilde{\rho}^\tau(t)).$$

This implies that, for any $\xi \in \text{Lip}_1$ and for every $\xi \in \text{Lip}_1$, we have

$$\langle \partial_t \tilde{\rho}_n(t), p_n(t) - \xi \rangle \leq \langle f_n(t), p_n(t) - \xi \rangle \quad \text{a.e. } t \in [0, T].$$

Using the fact that $p_n \partial_t \tilde{\rho}_n \geq 0$, we obtain

$$(3.30) \quad -\langle \partial_t \tilde{\rho}_n(t), \xi \rangle \leq \langle f_n(t), p_n(t) - \xi \rangle \quad \text{a.e. } t \in [0, T].$$

Finally, using the convergences (3.3), and (3.3) and passing to the limit as $\tau \rightarrow 0$ in (3.2), we deduce that the pair (ρ, p) satisfies (3.1). Finally, using (3.2), we see that

$$\frac{d}{dt} \langle \tilde{\rho}_n \rangle = \langle f_n \rangle, \quad \text{in } \mathcal{D}'(0, T),$$

so that letting $n \rightarrow \infty$, and using (3.3), we get (3.2). The conservation of mass for ρ_2 , (3.2), is directly derived from (3.2) and the fact that $\frac{d}{dt} \langle \rho_1 \rangle = \langle f \rangle$, in $\mathcal{D}'(0, T)$. \square

4. Algorithm and numerical computation

4.1. Algorithms. In this section, we focus on the development of a numerical algorithm to calculate the solutions to the congested pedestrian traffic flow model in crossings introduced in the previous sections. The core of our approach lies in a prediction-correction scheme, adapted here for the case of two distinct populations. This methodology builds on

the work of Maury and al. [33] and Ennaji and al. [21], who previously used this approach to model congestion in crowd motion for a single population.

For a given time-step $\tau > 0$, and a τ - discretization $0 = t_0 < t_1 < \dots < t_m = \tau[T/\tau] \leq T$, the prediction-correction algorithm divides the dynamics of the two populations, represented by densities ρ_1 and ρ_2 , into sequential steps on each interval $[t_k, t_{k+1}[$: a *prediction step* for ρ_1 followed by a *correction step* for ρ_2 .

Assuming that $\rho_1(t_k) =: \rho_{1,k}$ and $\rho_2(t_k) =: \rho_{2,k}$ are known at time $t = t_k$, with $\rho_{1,0} = \rho_{01}$ and $\rho_{2,0} = \rho_{02}$, we now describe the focus of each step:

Prediction step: This step focuses mainly on the computation of $\rho_{1,k+1}$ transporting the population ρ_1 through a spontaneous velocity field. To achieve this, we utilize the transport equation i.e.

$$(4.1) \quad \begin{cases} \frac{d\rho_1}{dt} + \nabla \cdot (\rho_1 V) = 0, & \text{in } [t_k, t_{k+1}) \times \Omega \\ \rho_1(t_k) = \rho_{1,k}, & \text{in } \Omega, \end{cases}$$

where V is derived from a potential, $V = -\nabla\varphi$. Then, we consider

$$\rho_{1,k+1} = \rho_1(t_{k+1}).$$

We consider three primary scenarios for determining V , as outlined in Remark 1:

- Directed movement: the potential φ is given by the geodesics towards the exit ; i.e. taking V definitely given by $V = -\nabla\varphi$, where the potential φ is given by the solution of the Eikonal equation:

$$(4.2) \quad \begin{cases} \|\nabla\varphi\| = 1 & \text{in } \Omega, \\ \varphi = 0 & \text{on } \Gamma_D. \end{cases}$$

Recall that the solution of equation (4.1) (in the viscosity sense) gives the fast path to the exit Γ_D . The potential φ corresponds to the expected travel time to maneuver towards an exit.

- Non-local interaction: the potential φ is non-local and is computed by the convolution of the solution with a Gaussian kernel, taking into account the influence of neighboring individuals. Within the time interval $[t_k, t_{k+1}[$, φ is given by

$$(4.3) \quad \varphi := \rho_1^k \star K_\sigma.$$

Here K_σ is the Gaussian kernel, accounting for the influence of neighboring individuals. Here

$$K_\sigma^\mu(x) = \frac{1}{\sigma\sqrt{2\pi}} \exp\left(-\frac{(x-\mu)^2}{2\sigma^2}\right),$$

where $\sigma > 0$ is the standard deviation, which measures the spread or dispersion of the distribution (larger standard deviation indicates a wider, flatter curve), and μ is the mean, or average, of the distribution (it represents the center of the bell curve).

- Diffusion-based interaction: the potential φ is obtained by solving a stationary PDE with the Laplacian operator :

$$\begin{cases} -\Delta\varphi = \rho_1^k & \text{in } \Omega \\ \varphi = 0 & \text{on } \partial\Omega. \end{cases}$$

This enables to capture diffusion-like interactions within the population. This is analogous to considering the vector field potential from equation (4.1), where we effectively replace K_σ with the Green's function to model a form of Brownian interaction that respects Dirichlet the boundary conditions.

Correction step: Since the prediction step may result in a density $\rho_{1,k+1}$ that violates the constraint; i.e. $\text{ess sup}_x(\rho_{1,k+1}(x) + \rho_{2,k}(x)) > 1$, we implement a correction step to adjust $\rho_{2,k}$ and ensure that the total population density remains within the permissible bounds. While, (3.1) may not be ideal for the theoretical study of the dynamics, as discussed earlier, it proves to be quite effective for numerical simulations in the correction phase, as we'll see below. More precisely, to achieve the correction we use the Euler-Implicit schema associated with the dynamic.

$$(4.4) \quad \begin{cases} \frac{d\rho_2}{dt} + \partial\mathbb{I}_{\text{Lip}_1}(p) \ni 0, & \text{in } [t_k, t_{k+1}) \\ p \geq 0, 0 \leq \rho_2 \leq 1 - \rho_1, p(\underbrace{1 - \rho_{1,k+1} - \rho_2}_{=:\kappa_k}) = 0, & \text{in } Q \\ \rho_2(t_k) = \rho_{2,k} & \text{in } \Omega. \end{cases}$$

This formulation has the advantage of aligning the dynamics with the framework employed in the work of [21], which has demonstrated excellent numerical performance in the context of congestion for a single population. However, in contrast to the single-population case where the critical density is fixed at 1, here we use a spatially dependent maximum density value, $\kappa_k(x)$ where $0 \leq \kappa \leq 1$. This function, assumed to be given, accounts for potential variations for the population ρ_2 in the maximum allowable density over space (and time).

To compute the solution (4.1), we use the associate Euler-Implicit schema associated with (4.1), at the step k . That is

$$(4.5) \quad \begin{cases} \rho_{2,k+1} + \partial\mathbb{I}_{\text{Lip}_1}(p_{k+1}) = \rho_{2,k}, \\ p_{2,k+1} \geq 0, 0 \leq \rho_{2,k+1} \leq \kappa_k, p_{2,k+1}(\kappa_k - \rho_{2,k+1}) = 0, \end{cases}$$

with $\rho_{2,0} = \rho_{02}$ given.

Using the 1-Wasserstein distance, W_1 , and the concept of the Kantorovich potential as in the study of the problem (3.1), it is not difficult to see that, the solution of the discrete problem (4.1) is also given by

$$(4.6) \quad p_{k+1} \in \mathcal{K}(\rho_{2,k} - \rho_{2,k+1}), \quad 0 \leq \rho_{2,k+1} \leq \kappa_k, \quad 0 \leq p_{k+1}, p_{k+1}(\kappa_k - \rho_{2,k+1}) = 0.$$

That is $p_{k+1} \in \text{Lip}_1$ and

$$\langle \rho_{2,k} - \rho_{2,k+1}, p_{k+1} - \psi \rangle \geq 0, \quad \forall \psi \in \text{Lip}_1,$$

with

$$0 \leq \rho_{2,k+1} \leq \kappa_k, \quad 0 \leq p_{k+1}, \quad p_{k+1}(1 - \rho_{2,k+1}) = 0.$$

Following the same proof of Lemma 3.1, we have the following result where we replace the density maximal value 1, by space dependent value κ_k .

LEMMA 4.4. *Given a time step $\tau > 0$, for any $k = 1, \dots, m$, the sequences $\rho_k^{2,\tau}$ and p_k^τ in (4.1) are well defined inductively by*

$$\rho_{2,k}^\tau \in \operatorname{argmin}_u \left\{ W_1(\rho_{2,k-1}^\tau - u) : \langle \rho_{2,k-1}^\tau - u \rangle = 0, u \in L^\infty(\Omega), 0 \leq u \leq \kappa_k \right\},$$

and

$$p_k^\tau \in \operatorname{argmax}_\theta \left\{ \langle \rho_{2,k-1}^\tau, \theta \rangle - \int \kappa_k \theta : 0 \leq \theta \in \text{Lip}_1 \right\}$$

by setting $\rho_{2,0}^\tau = \rho_{02}$. Moreover, we have

$$(4.7) \quad \rho_k^\tau \in \operatorname{argmin}_u \inf_{\sigma \in (L^\infty(\Omega)')^N} \left\{ \|\sigma\|_{(L^\infty(\Omega)')^N} : \langle \sigma, \nabla \xi \rangle = \int_\Omega (\rho_{2,k-1}^\tau - u) \xi dx, \right.$$

$$\left. \forall \xi \in \text{Lip}_1, u \in L^\infty(\Omega), 0 \leq u \leq \kappa_k \right\},$$

where the duality bracket is taken in the sense of $((L^\infty(\Omega)')^N, L^\infty(\Omega)^N)$.

PROOF. The proof follows by adapting the techniques employed in Lemma 3.1. In this case, we replace the constraint $0 \leq u \leq 1$, by a spatially varying constraint of the form $0 \leq u \leq \kappa_k$. Subsequently, the duality result expressed in (4.4) follows from the fact

$$W_1(\rho_{2,k-1}^\tau - u) = \inf_{\sigma \in (L^\infty(\Omega)')^N} \left\{ \|\sigma\|_{(L^\infty(\Omega)')^N} : \langle \sigma, \nabla \xi \rangle = \int_\Omega (\rho_{2,k-1}^\tau - u) \xi dx, \quad \forall \xi \in \text{Lip}_1 \right\}.$$

□

Coming back to the computation of ρ_2^{k+1} in the correction step through the scheme (4.1), we use Lemma 4.4 and proceed with a minimum flow process in (4.4). More precisely, we consider ρ_2^{k+1} to be the solution to the following regularized optimization problem:

$$(4.8) \quad \operatorname{argmin}_u \inf_\sigma \left\{ \int_\Omega |\sigma|(x) dx : \int_\Omega \sigma \cdot \nabla \xi dx = \int_\Omega (\rho_{2,k-1}^\tau - u) \xi dx, \right.$$

$$\left. \forall \xi \in \text{Lip}_1, u \in L^\infty(\Omega), 0 \leq u \leq \kappa_k \right\}$$

This formulation allows to update the density ρ_2 while respecting the constraint $\rho_1 + \rho_2 \leq 1$, and at the same time to optimize the velocity field σ to adjust the dynamics of the system. This vector field, σ , represents the flow rate used by population ρ_2 to relieve congestion.

4.2. Numerical approximation: As mentioned in the previous section, the approximation of the densities ρ_1 and ρ_2 is performed using a prediction correction strategy. The first step, called prediction, consists of solving the transport equation (4.1) using an Euler scheme for time discretization, while the term $\text{div}(\rho_1 V_1)$ is discretized using the finite volume method. The second step, correction or projection, involves a minimum flow problem, which will be solved using a primal-dual (PD) algorithm. To begin, we will detail the discretization of the problems (4.1) and (4.1).

Domain Discretization: In this section, we numerically solve equations (4.1) and (4.1) over the domain Ω . This domain represents a room surrounded by walls, denoted as Γ_N , and featuring an exit door Γ_D . The domain is divided into $m \times n$ control volumes, each with a length and width of h . We define $C_{i,j}$ as the cell located at position (i, j) , and $\Psi_{i,j}$ as the average value of the quantity Ψ within cell $C_{i,j}$. At the boundaries of cell $C_{i,j}$, $\omega_{i+1,j}$ and $\omega_{i,j-1}$ represent the in-flow and out-flow quantities, respectively.

Discretization of the Operators: The space $X = \mathbb{R}^{m \times n}$ is equipped with a scalar product and an associated norm as follows:

$$\langle u, v \rangle = h^2 \sum_{i=1}^m \sum_{j=1}^n u_{i,j} v_{i,j}, \quad \|u\|^2 = \langle u, u \rangle.$$

For $1 \leq i \leq m$ and $1 \leq j \leq n$, we define the components of the discrete gradient operator via finite differences:

$$(\nabla_h u)_{i,j}^1 = \begin{cases} \frac{u_{i+1,j} - u_{i,j}}{h} & \text{if } i < m, \\ 0 & \text{if } i = m. \end{cases}$$

$$(\nabla_h u)_{i,j}^2 = \begin{cases} \frac{u_{i,j+1} - u_{i,j}}{h} & \text{if } j < n, \\ 0 & \text{if } j = n. \end{cases}$$

Then, the discrete gradient $\nabla_h : X \rightarrow Y = \mathbb{R}^{m \times n \times 2}$ is given by:

$$(\nabla_h u)_{i,j} = ((\nabla_h u)_{1,i,j}, (\nabla_h u)_{2,i,j}).$$

Similar to the continuous setting, we define a discrete divergence operator $\text{div}_h : Y \rightarrow X$, which is the minus of the adjoint of ∇_h , given by $\text{div}_h = -\nabla_h^*$. That is,

$$\langle -\text{div}_h \phi, u \rangle_X = \langle \phi, \nabla_h u \rangle_Y \quad \text{for any } \phi = (\phi_1, \phi_2) \in Y \quad \text{and } u \in X.$$

It follows that the divergence with homogeneous Neuman boundary condition is explicitly given by:

$$\text{div}_h \phi_{i,j} = \begin{cases} \frac{\phi_{1i,j}}{h} & \text{if } i = 1, \\ \frac{\phi_{1i,j} - \phi_{1i-1,j}}{h} & \text{if } 1 < i < m, \\ -\frac{\phi_{1m-1,j}}{h} & \text{if } i = m, \end{cases} + \begin{cases} \frac{\phi_{2i,j}}{h} & \text{if } j = 1, \\ \frac{\phi_{2i,j} - \phi_{2i,j-1}}{h} & \text{if } 1 < j < n, \\ -\frac{\phi_{2i,n-1}}{h} & \text{if } j = n. \end{cases}$$

Discretization of the transport equation (2.1): We apply a splitting method as follows. Given an end time $T > 0$ and a timestep $\tau > 0$, we decompose the interval $[0, T]$ into subintervals $[t_k, t_{k+1}]$ and $[t_{k+1}, t_{k+1}]$, with $k = 0, \dots, n-1$. On each interval $[t_k, t_{k+1}]$, we solve the transport equation (4.1) to obtain $\rho_{1,k+1}$, where $V = (V_x, V_y)$ is the velocity field given by $V = -\nabla D$, and D is given by one of the scenarios we describe above. In the case where D is the distance to the boundary Γ_D , we solve the Eikonal equation (4.1) using the variational method as described in Appendix-B of the work [21]. Solving (4.1) is done by combining a finite difference method in time with a 2D finite volume method in space. We approximate the term $\text{div}(V_1 \rho_1)$ in the cell $C_{i,j} = [x_{i-1/2}, x_{i+1/2}] \times [y_{i,j-1}, y_{i,j+1/2}]$ as follows:

$$\begin{aligned} (\text{div}(V_1 \rho_1))_{i,j} &= \frac{1}{\Delta x} \left[F_{\text{up}} \left(V_{i+\frac{1}{2},j}^x, \rho_{i+\frac{1}{2},j}^k, -\rho_{i+\frac{1}{2},j}^k \right) - F_{\text{up}} \left(V_{i-\frac{1}{2},j}^x, \rho_{i-\frac{1}{2},j}^k, -\rho_{i-\frac{1}{2},j}^k \right) \right] \\ &\quad + \frac{1}{\Delta y} \left[F_{\text{up}} \left(V_{i,j+\frac{1}{2}}^y, \rho_{i,j+\frac{1}{2}}^k, -\rho_{i,j+\frac{1}{2}}^k \right) - F_{\text{up}} \left(V_{i,j-\frac{1}{2}}^y, \rho_{i,j-\frac{1}{2}}^k, -\rho_{i,j-\frac{1}{2}}^k \right) \right]. \end{aligned}$$

We consider in this discretisation $\rho = \rho_1$, and $(\text{div}(V \rho_1))_{i,j}$ is the value of $\text{div}(V_1 \rho_1)$ in the cell $C_{i,j}$, $(\Delta x, \Delta y)$ are the spatial discretizations.

$$F_{\text{up}}(x, y, z) = \begin{cases} xy & \text{if } x \geq 0, \\ xz & \text{if } x < 0. \end{cases}$$

For the time discretization, we use the Euler explicit method to approximate the time derivative of the density. The overall scheme can be written as:

$$\begin{aligned} \frac{\rho_{i,j}^{k+1} - \rho_{i,j}^k}{\tau} + \frac{1}{\Delta x} \left(F_{\text{up}}(V_{i+\frac{1}{2},j}^x, \rho_{i+\frac{1}{2},j}^k, \rho_{i+\frac{1}{2},j}^k, \rho_{i-\frac{1}{2},j}^k) - F_{\text{up}}(V_{i-\frac{1}{2},j}^x, \rho_{i-\frac{1}{2},j}^k, \rho_{i-\frac{1}{2},j}^k, \rho_{i,j}^k) \right) \\ + \frac{1}{\Delta y} \left(F_{\text{up}}(V_{i,j+\frac{1}{2}}^y, \rho_{i,j+\frac{1}{2}}^k, \rho_{i,j+\frac{1}{2}}^k, \rho_{i,j-\frac{1}{2}}^k) - F_{\text{up}}(V_{i,j-\frac{1}{2}}^y, \rho_{i,j-\frac{1}{2}}^k, \rho_{i,j-\frac{1}{2}}^k, \rho_{i,j}^k) \right) = 0. \end{aligned}$$

where $\rho_{i,j}^{k+1}$ is the average value of ρ_1 in the cell $C_{i,j} = [x_{i-\frac{1}{2},j}, x_{i+\frac{1}{2},j}] \times [y_{i,j-\frac{1}{2}}, y_{i,j+\frac{1}{2}}]$ at time $(k+1)\tau$, and $\rho_{a,b}^k, V_{a,b}^x$ (respectively $V_{a,b}^y$) are the values of ρ_1 and V at the interface $x_{a,b}$ (respectively $y_{a,b}$) at time $k\tau$. Notice that in practice, we take $\Delta x = \Delta y = h$, where h is the mesh size introduced above.

Using the upwind scheme we have and substituting in (4.2), the density $\rho_{i,j}^{k+1}$ can be written as ([33]):

$$\begin{aligned} \rho_{i,j}^{k+1} &= \rho_{i,j}^k - \frac{\tau}{h} \left(F_{\text{up}}(V_{i+\frac{1}{2},j}^x, \rho_{i,j}^k, \rho_{i-1,j}^k) - F_{\text{up}}(V_{i-\frac{1}{2},j}^x, \rho_{i-1,j}^k, \rho_{i,j}^k) \right) \\ &\quad - \frac{\tau}{h} \left(F_{\text{up}}(V_{i,j+\frac{1}{2}}^y, \rho_{i,j}^k, \rho_{i,j-1}^k) - F_{\text{up}}(V_{i,j-\frac{1}{2}}^y, \rho_{i,j-1}^k, \rho_{i,j}^k) \right). \end{aligned}$$

We consider that no flux is entering the room from the boundary at $\partial\Omega$. This is equivalent to impose $\rho_{i-\frac{1}{2},j}^k V_{i-\frac{1}{2},j}^x = 0$ and $\rho_{i,j-\frac{1}{2}}^k V_{i,j-\frac{1}{2}}^y = 0$ at $i = 1$ and $j = 1$ respectively. The scheme (4.2) is conservative, stable under the CFL condition $\|V\|_{\infty} \frac{\tau}{h} \leq \frac{1}{2}$. This condition

can be obtained using von Neumann stability analysis (cf. [16, 18]). We summarize this in the following algorithm:

Algorithm 1: Prediction step

1st step. Initialization: Compute the velocity $\mathbf{V} = (V_x, V_y)$. Choose $\Delta x = \Delta y = h$ and τ such that

$$\|\mathbf{V}\|_\infty \frac{\tau}{h} \leq \frac{1}{2},$$

and take an initial density given by $\rho_{1,(i,j)}^k$ at time $k\tau$.

2nd step. Update the density: At time $(k+1)\tau$, update $\rho_{i,j}$ using:

$$\begin{aligned} \rho_{i,j}^{k+1} = & \rho_{i,j}^k - \frac{\tau}{h} \left(F_{\text{up}}(V_{i+\frac{1}{2},j}^x, \rho_{i,j}^k, \rho_{i-1,j}^k) - F_{\text{up}}(V_{i-\frac{1}{2},j}^x, \rho_{i-1,j}^k, \rho_{i,j}^k) \right) \\ & - \frac{\tau}{h} \left(F_{\text{up}}(V_{i,j+\frac{1}{2}}^y, \rho_{i,j}^k, \rho_{i,j-1}^k) - F_{\text{up}}(V_{i,j-\frac{1}{2}}^y, \rho_{i,j-1}^k, \rho_{i,j}^k) \right). \end{aligned}$$

Notice: In the case where $V_x > 0$ and $V_y > 0$, the update formula reduces to:

$$\rho_{i,j}^{k+1} = \rho_{i,j}^k - \frac{\tau}{\Delta x} \left[\rho_{i,j}^k V_{i+\frac{1}{2},j}^x - \rho_{i-1,j}^k V_{i-\frac{1}{2},j}^x \right] - \frac{\tau}{\Delta y} \left[\rho_{i,j}^k V_{i,j+\frac{1}{2}}^y - \rho_{i,j-1}^k V_{i,j-\frac{1}{2}}^y \right].$$

Discretization of the correction : When calculating ρ_1^{k+1} , which moves and may cause a sum with ρ_2^k to be greater than 1, we need to adjust ρ_2^k to ensure that the constraint $\rho_1 + \rho_2 \leq 1$ is met. Thus, the next step is to deal with congestion by solving the following minimum flow problem (4.1). where $\kappa_k = 1 - \rho_1^{k+1}$.

First, let us rewrite (4.1) in the form :

$$(\mathbf{M}) : \min_{\rho_2, \Phi_2} A(\rho_2, \Phi_2) + \mathbb{I}_C(\Lambda(\rho_2, \Phi_2)),$$

where (we omit the variable τ to lighten the notation)

$$A(\rho_2, \Phi_2) = \int_{\Omega} \tau |\Phi_2(x)| dx + \mathbb{I}_{[0,\kappa]}(\rho_2),$$

$$\Lambda(\rho_2, \Phi_2) = \rho_2 - \tau \operatorname{div}(\Phi_2),$$

and

$$B = \mathbb{I}_{\rho_2^k}.$$

Here, \mathbb{I}_C is the indicator function of the set C , and it is given by:

$$\mathbb{I}_C(a) = \begin{cases} 0 & \text{if } a \in C, \\ +\infty & \text{if } a \notin C. \end{cases}$$

This problem can be solved efficiently using the Chambolle-Pock's primal-dual (PD) algorithm (cf. [14]). Based on the discrete gradient and divergence operators, we propose a discrete version of (M) as follows:

$$(M)_d : \min_{\rho_2, \Phi_2} \left\{ h^2 \sum_{i=1}^{m+1} \sum_{j=1}^{n+1} \tau \|\Phi_{2,i,j}\| + \mathbb{I}_{[0,\kappa]}(\rho_2) + \mathbb{I}_{\mathcal{C}}(\Lambda_h(\rho_2, \Phi_2)) \right\},$$

where

$$\mathcal{C} := \left\{ (a_{i,j}) : a_{i,j} = \rho_{(i,j)}^k, \forall (i,j) \in \llbracket 1, m \rrbracket \times \llbracket 1, n \rrbracket, \Lambda_h(\rho_2, \phi_2) = \rho_2 - \tau \operatorname{div}_h \Phi_2 \right\}.$$

In other words, the discrete version (M)_d can be written as

$$\min_{\rho_2, \Phi_2} \mathcal{A}_h(\rho_2, \Phi_2) + \mathcal{B}_h(\Lambda_h(\rho_2, \Phi_2)),$$

or in a primal-dual form as

$$\min_{\rho_2, \Phi_2} \max_p \mathcal{A}_h(\rho_2, \Phi_2) + \langle u, \Lambda_h(\rho_2, \Phi_2) \rangle - \mathcal{B}_h^*(p),$$

where

$$\mathcal{A}_h(\rho_2, \Phi_2) = h^2 \sum_{i=1}^{m+1} \sum_{j=1}^{n+1} \tau \|\phi_{2,i,j}\| + \mathbb{I}_{[0,\kappa]}(\rho_2) \quad \text{and} \quad \mathcal{B}_h = \mathbb{I}_{\mathcal{C}}.$$

Notice that in this case, (2.29) has a dual problem that reads:

$$\min_{\rho_2} \max_p h^2 \left\{ \sum_{i=1}^m \sum_{j=1}^n p_{i,j} \left(\rho_{i,j}^{k+1} - \rho_{i,j} \right) : \|\nabla_h p_{i,j}\| \leq 1, 0 \leq \rho_2 \leq \kappa \right\}.$$

Then the (PD) algorithm ([15]) can be applied to (M)_d as follows:

Algorithm 2: (PD) iterations

1st step. Initialization: Choose $\alpha, \beta > 0$, $\theta \in [0, 1]$, ρ_2^0, Φ_2^0 , and take $u_0 = \Lambda_h(\rho_2^0, \Phi_2^0), \bar{p}_0$.

2nd step. For $l \leq \text{Itermax}$, **do:**

$$(\rho_2^{l+1}, \Phi_2^{l+1}) = \operatorname{Prox}_{\beta \mathcal{A}_h} \left((\rho_2^l, \Phi_2^l) - \beta \Lambda_h^*(\bar{p}_l) \right);$$

$$p_{l+1} = \operatorname{Prox}_{\alpha \mathcal{B}_h^*} \left(p_l + \alpha \Lambda_h(\rho_2^{l+1}, \Phi_2^{l+1}) \right);$$

$$\bar{p}_{l+1} = p_{l+1} + \theta (p_{l+1} - p_l).$$

Let us recall that the proximal operator is defined as follows:

$$\operatorname{Prox}_{\alpha E}(p) = \operatorname{argmin}_q \left(\frac{1}{2} \|p - q\|^2 + \eta E(q) \right).$$

Computation of the proximal operators

Note that the functionals \mathcal{A}_h and \mathcal{B}_h^* can be computed explicitly. Specifically, the functional \mathcal{A}_h is separable in terms of the variables ρ_2 and Φ_2 :

$$\mathcal{A}_h(\rho_2, \Phi_2) = \mathbb{I}_{[0,1-\rho_1]}(\rho_2) + \|\Phi_2\|_1.$$

Therefore, $\text{Prox}_{\eta\mathcal{A}_h}$ consists of the sum of a projection onto the first component and the so-called soft-thresholding. More explicitly:

$$(\text{Prox}_{\mathcal{A}_h}(\rho_2, \Phi_2))_{i,j} = \left(\max\left(0, \min\left(1 - \rho_{1,(i,j)}, \rho_{(i,j)}\right)\right), \max\left(0, 1 - \frac{1}{|\Phi_{2,(i,j)}|}\right) \Phi_{2,(i,j)} \right).$$

For \mathcal{B}_h^* , in order to compute $\text{Prox}_{\alpha\mathcal{B}_h^*}$, we apply Moreau's identity:

$$p = \text{Prox}_{\alpha\mathcal{B}_h^*}(p) + \alpha\text{Prox}_{\alpha^{-1}\mathcal{B}_h}(p/\eta),$$

and note that $\text{Prox}_{\alpha^{-1}\mathcal{B}_h}(a, b)$ is simply the projection onto \mathcal{C} . Hence, we have:

$$\left(\text{Prox}_{\alpha\mathcal{B}_h^*}(p)\right)_{i,j} = \left(p_{i,j} - \alpha\text{Proj}_{\mathcal{C}_{i,j}}(p_{i,j}/\alpha)\right).$$

In summary, the steps in **Algorithm 3** to solve $(M)_d$ are as follows:

Algorithm 3 (PD) iterations for $(M)_d$

Initialization: Let $k = 0$, choose $\alpha, \beta > 0$ such that $\alpha\beta\|\Lambda_h\|^2 < 1$. Choose $\rho_1^0, \rho_2^0, \Phi_2^0$, and $p^0 = \bar{p}^0 = p_0$.

Primal step:

$$\left(\rho_2^{l+1}\right)_{i,j} = \max\left(0, \min\left(1 - \rho_{1,i,j}^l, \rho_{i,j}^l - \beta\bar{p}_{i,j}^l\right)\right),$$

and

$$\left(\Phi_2^{l+1}\right)_{i,j} = \max\left(0, 1 - \frac{1}{|\Phi_{2,i,j}^l - \beta\nabla_h\bar{p}_{i,j}^l|}\right) \left(\Phi_{2,i,j}^l - \beta\nabla_h\bar{p}_{i,j}^l\right).$$

Dual step:

$$v^{l+1} = p^l + \alpha\rho_2^{l+1} - \alpha\text{div}_h\left(\Phi_2^{l+1}\right),$$

$$p_{i,j}^{l+1} = v_{i,j}^{l+1} - \alpha\text{Proj}_{\mathcal{C}_{i,j}}\left(v_{i,j}^{l+1}/\alpha\right), \quad 1 \leq i \leq m, \quad 1 \leq j \leq n.$$

Extragradient:

$$\bar{p}^{l+1} = 2p^{l+1} - p^l.$$

4.3. Numerical computation: This section presents several illustrative examples. The first three cases consider a transport equation where the vector field V is defined by a specific destination, inducing directed motion in population 1 and compelling population 2 to adapt its distribution to accommodate spatial constraints. Examples 4 – 7 explore

scenarios where the transport vector field is determined by a non-local potential, enabling population 1 to disperse based on local neighborhood influences through Gaussian convolution. In contrast to previous cases where boundary conditions were inherent to the vector field V , we now examine two types of boundary conditions: Dirichlet, allowing population members to exit the domain, and reflective, where individuals may or may not re-enter. Finally, in Examples 8 – 9 we numerically analyze a scenario where the potential field V is directly linked to the diffusion of population 1.

All computational codes were implemented in Python¹.

4.3.1. *Example 1:* A population ρ_1 is moving rightward and encounters a stationary population ρ_2 :

¹Demonstration videos are available at https://www.unilim.fr/pages_perso/noureddine.igbida/

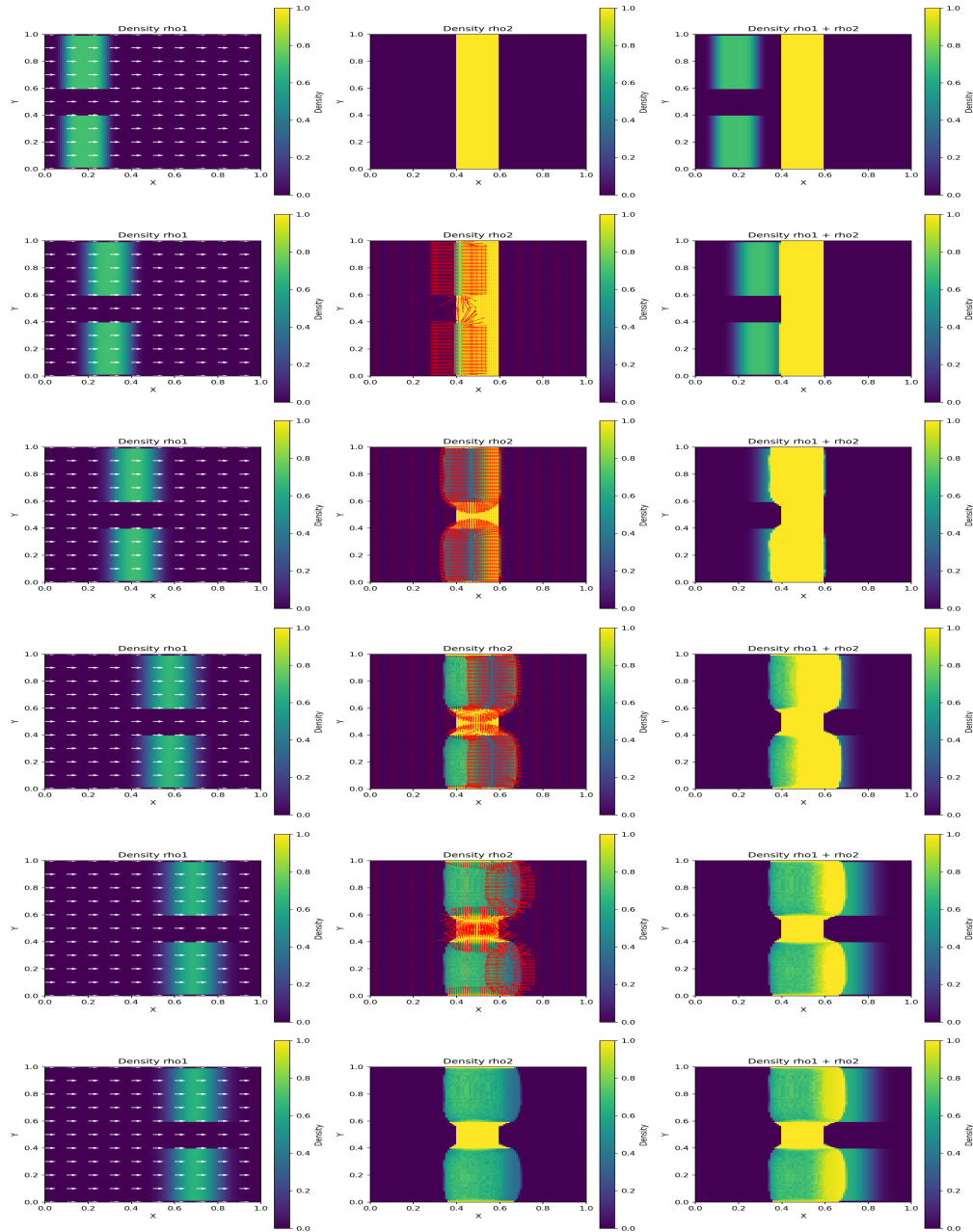


FIGURE 1. Snapshots of ρ_2 (left) moving along the red-patterned field, interacting with ρ_1 (moving along the white field, center). The right image visualizes the combined density $\rho_1 + \rho_2$. The red movement of population ρ_2 is only triggered when it encounters population ρ_1 and $\rho_1 + \rho_2 = 1$

4.3.2. *Example 2:* As in Example 1, the population ρ_1 is moving rightward and encounters a stationary population ρ_2 :

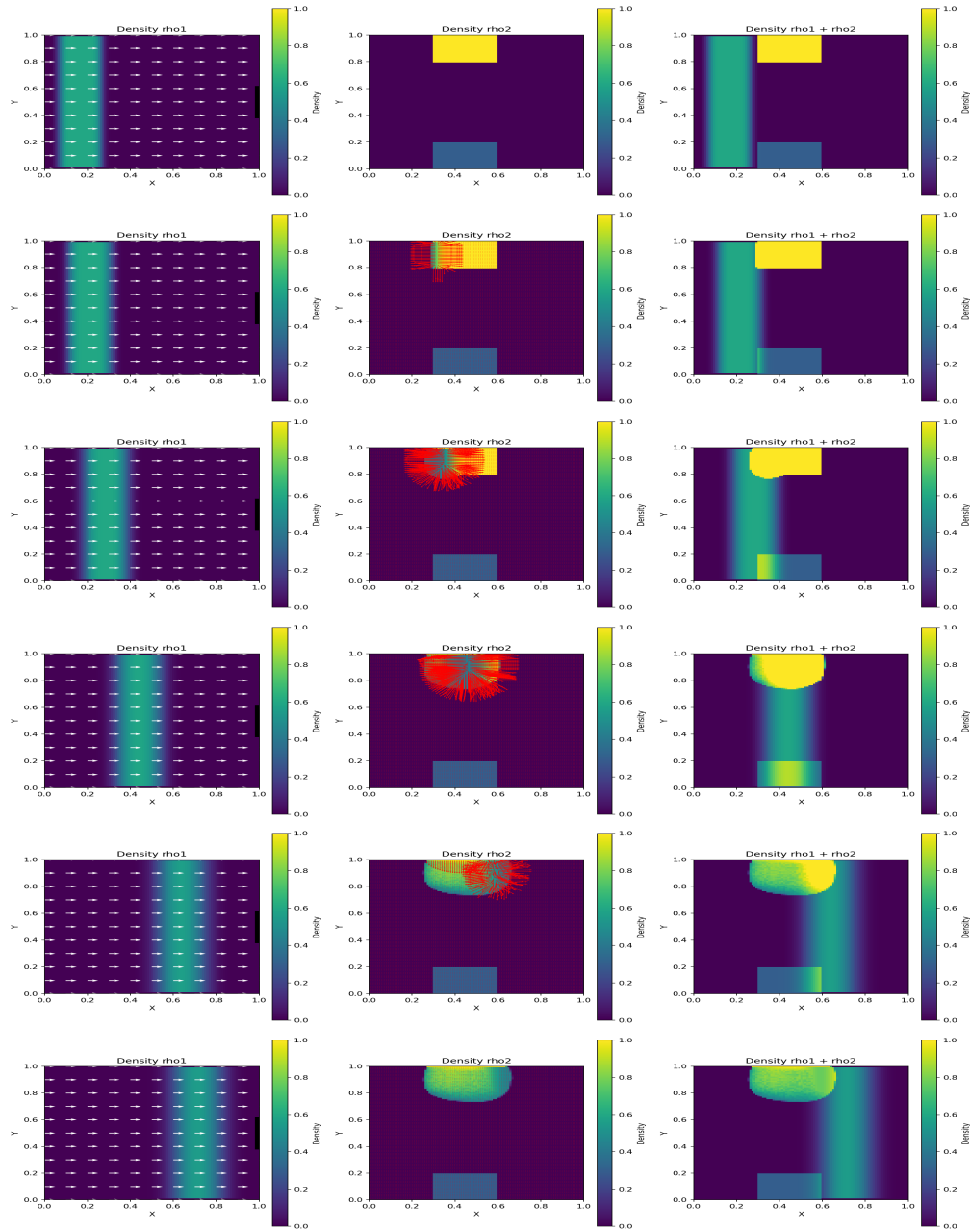


FIGURE 2. The absence of ρ_2 flux (red arrows) in the bottom block can be attributed to the enforcement of the maximum density constraint throughout the dynamical evolution.

4.3.3. *Example 3:* A rotating population ρ_1 meets a static population ρ_2 along its trajectory:

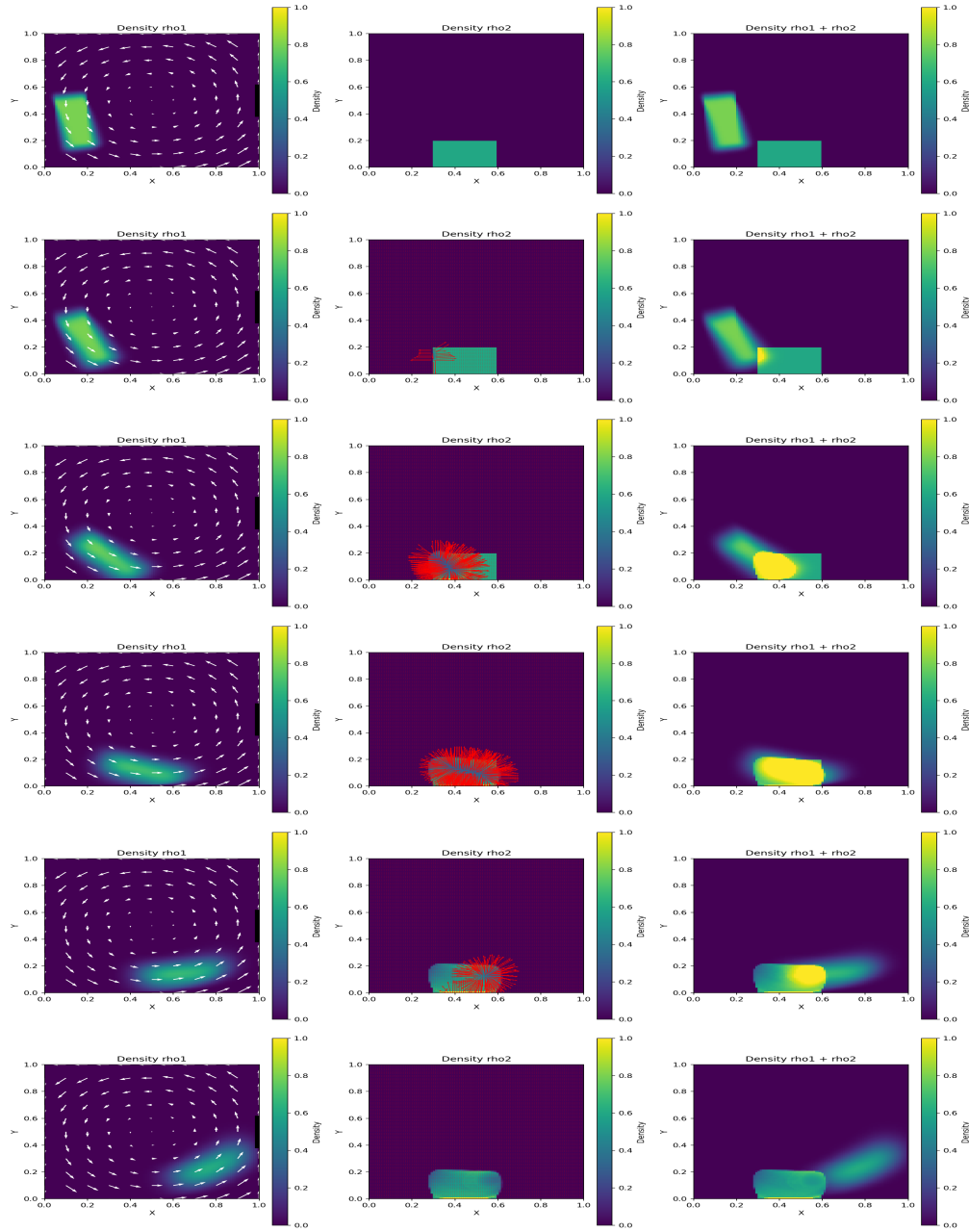


FIGURE 3. Snapshots of ρ_2 (left) rotating along the red-patterned field, interacting with ρ_1 (moving along the white field, center).

4.3.4. *Example 4:* A population ρ_1 spreads out to reduce density variations in its immediate surroundings through a Gaussian smoothing process. This expanding population eventually meets a stationary population ρ_2 surrounding it. The initial distribution of ρ_1 is a combination of four Gaussian peaks, and ρ_2 is simply the complement of ρ_1 . The convolution process effectively extends the domain of the population ρ_1 with zeros, forcing its members to leave the domain.

Data set

- $\rho_{01} = 0.9(K_\lambda^{\mu_1} + K_\lambda^{\mu_2} + K_\lambda^{\mu_3} + K_\lambda^{\mu_4})$ in $\Omega := [0, 1] \times [0, 1]$ with $\lambda = 0.1$, $\mu_1 = (0.3, 0.7)$, $\mu_2 = (0.7, 0.3)$, $\mu_3 = (0.3, 0.3)$ and $\mu_4 = (0.7, 0.7)$
- $\rho_{02} = 0.9(1 - \rho_{01})$.
- The vector field potential here is given by $\varphi = \rho_1 \star K_\sigma^\mu$, where $\sigma = 5$ and $\mu = (0, 0)$.

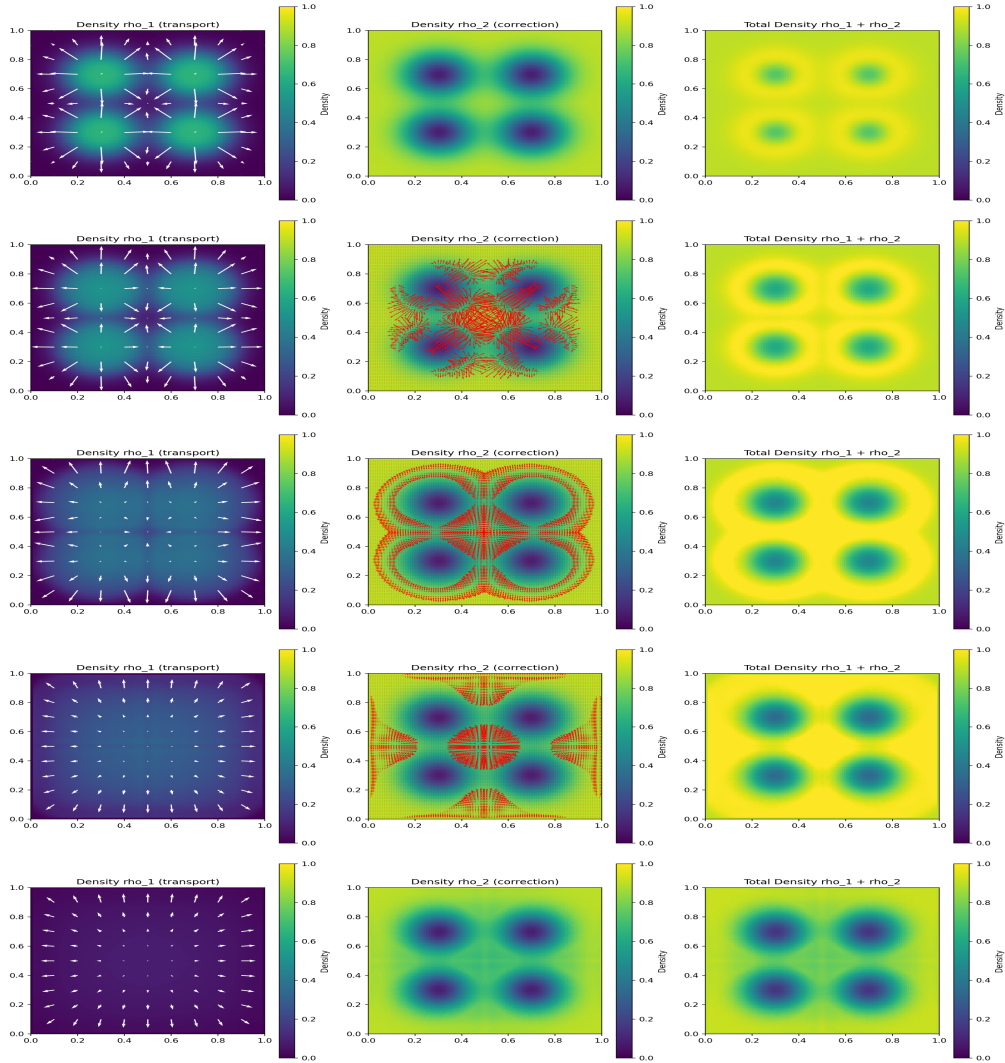


FIGURE 4. Snapshots of ρ_2 (left) moving along the red-patterned field, interacting with ρ_1 (moving along the white field, center). The right image visualizes the combined density $\rho_1 + \rho_2$. Population 2's red-indicated movement is triggered only when it encounters population ρ_1 and $\rho_1 + \rho_2 = 1$. By the end of the simulation, the entire population ρ_1 continues to leave the domain without congestion, and population ρ_2 is left with its final distribution from the previous time step.

4.3.5. *Example 5:* In this case, we use the same data set as in Example 4, but we modify the boundary condition. We implement a "reflect" type boundary condition that reflects the value closest to the boundary. This technique can be effectively used when a pedestrian reaches the boundary, instead of simply stopping or disappearing, the "reflect"

condition simulates a scenario where the pedestrian "bounces back" into the domain. This is achieved by mirroring the pedestrian density across the boundary.

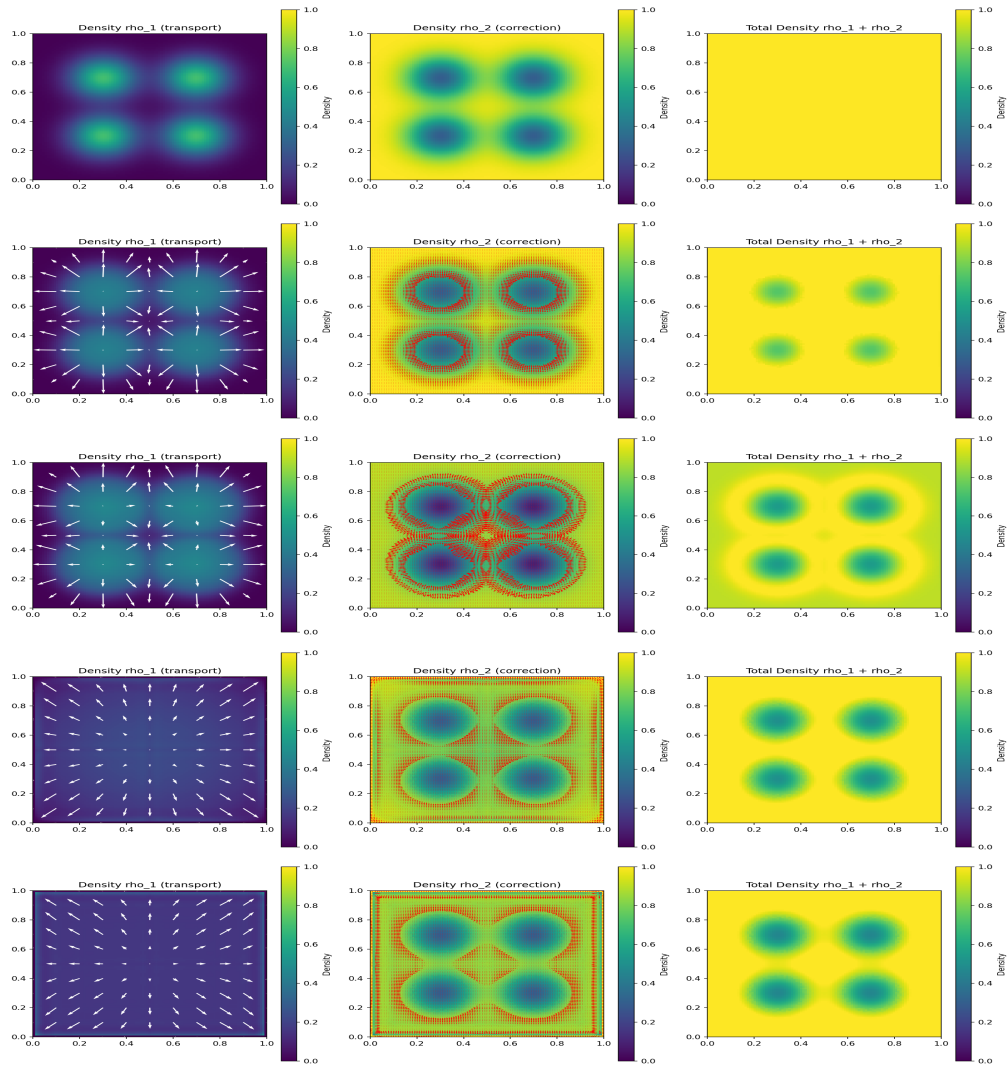


FIGURE 5. In contrast to the earlier scenario in Example 4, the reflective nature of the boundary conditions serves to preserve congestion within the domain upon population ρ_1 reaching the boundary.

4.3.6. *Example 6:* A scenario similar to Example 4 with three initial Gaussian distributions and zero-padding convolution which effectively forces population ρ_1 to exit the domain.

Data set

- $\rho_{01} = 0.5(K_\lambda^{\mu_1} + K_\lambda^{\mu_2} + K_\lambda^{\mu_3} + K_\lambda^{\mu_4})$ in $\Omega := [0, 1] \times [0, 1]$ with $\lambda = 0.1$, $\mu_1 = (0.2, 0.5)$, $\mu_2(0.5, 0.2)$, $\mu_3 = (0.5, 0.8)$
- $\rho_{02} = 0.9(1 - \rho_{01})$.
- The vector field potential here is given by $\varphi = \rho_1 \star K_\sigma^\mu$, where $\sigma = 5$ and $\mu = (0, 0)$.

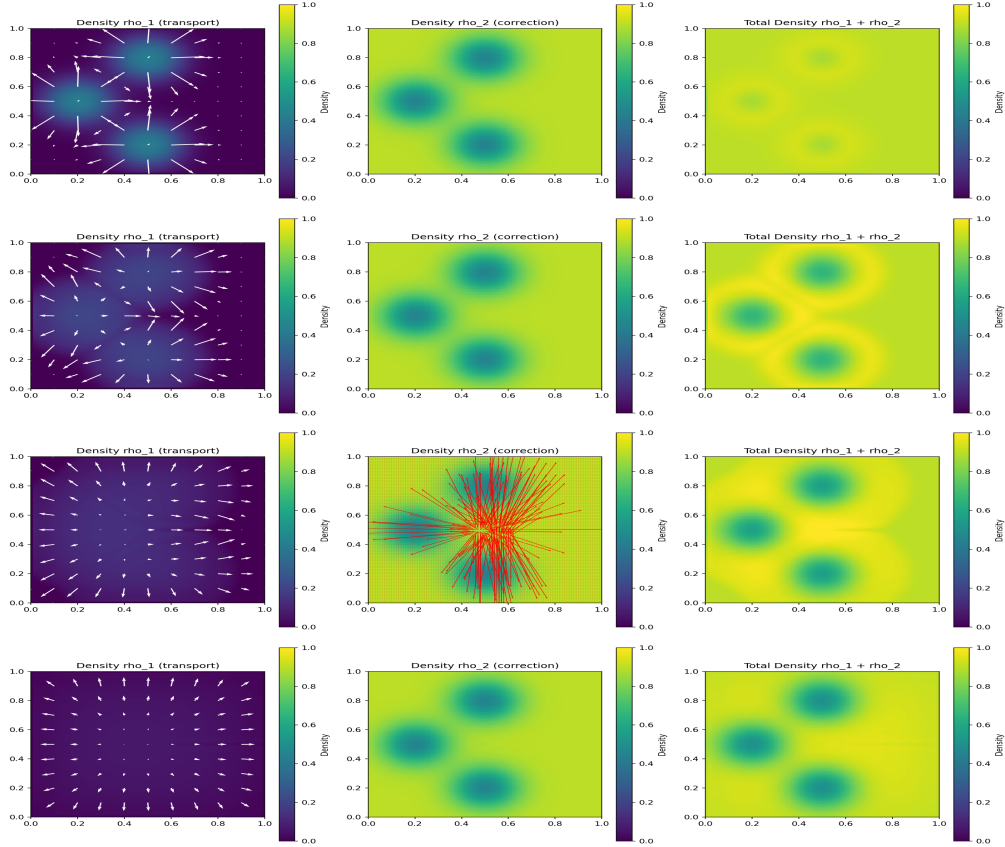


FIGURE 6. As in Fig. 4, by the end of the simulation, the entire population ρ_1 continues to leave the domain without any congestion.

4.3.7. *Example 7:* A scenario similar to Example 6, with the same data set, but we modify the boundary condition by implementing "reflect" boundary conditions.

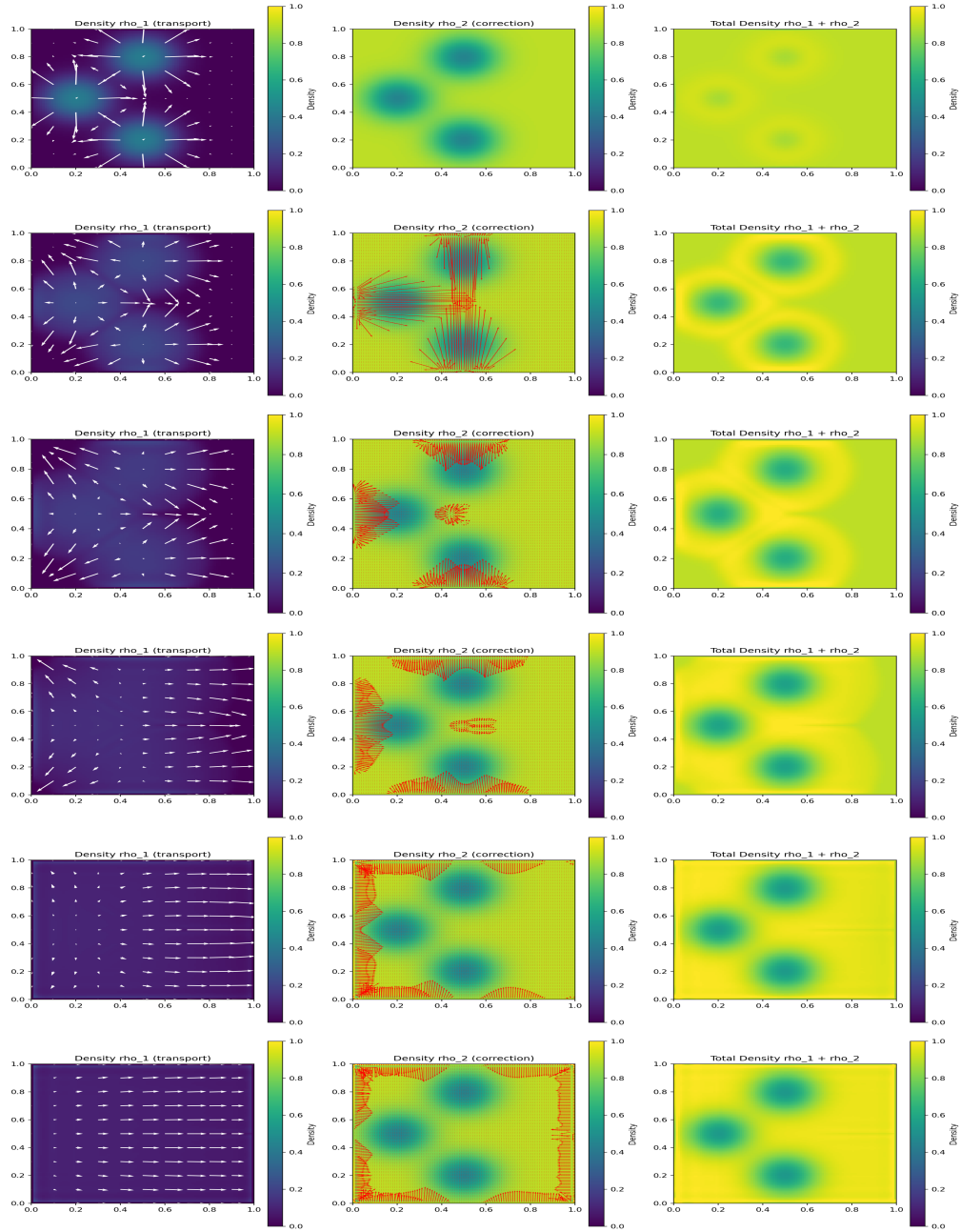


FIGURE 7. Unlike the previous case, the boundary conditions lead to a persistent congestion near the boundary due to the inward reflection of the population.

4.3.8. *Example 8:* Population ρ_1 , with an initial distribution of a Gaussian function, undergoes diffusion with Dirichlet boundary conditions. This leads to population expansion and eventual exit from the domain, while population ρ_2 , initially surrounding ρ_1 , remains confined.

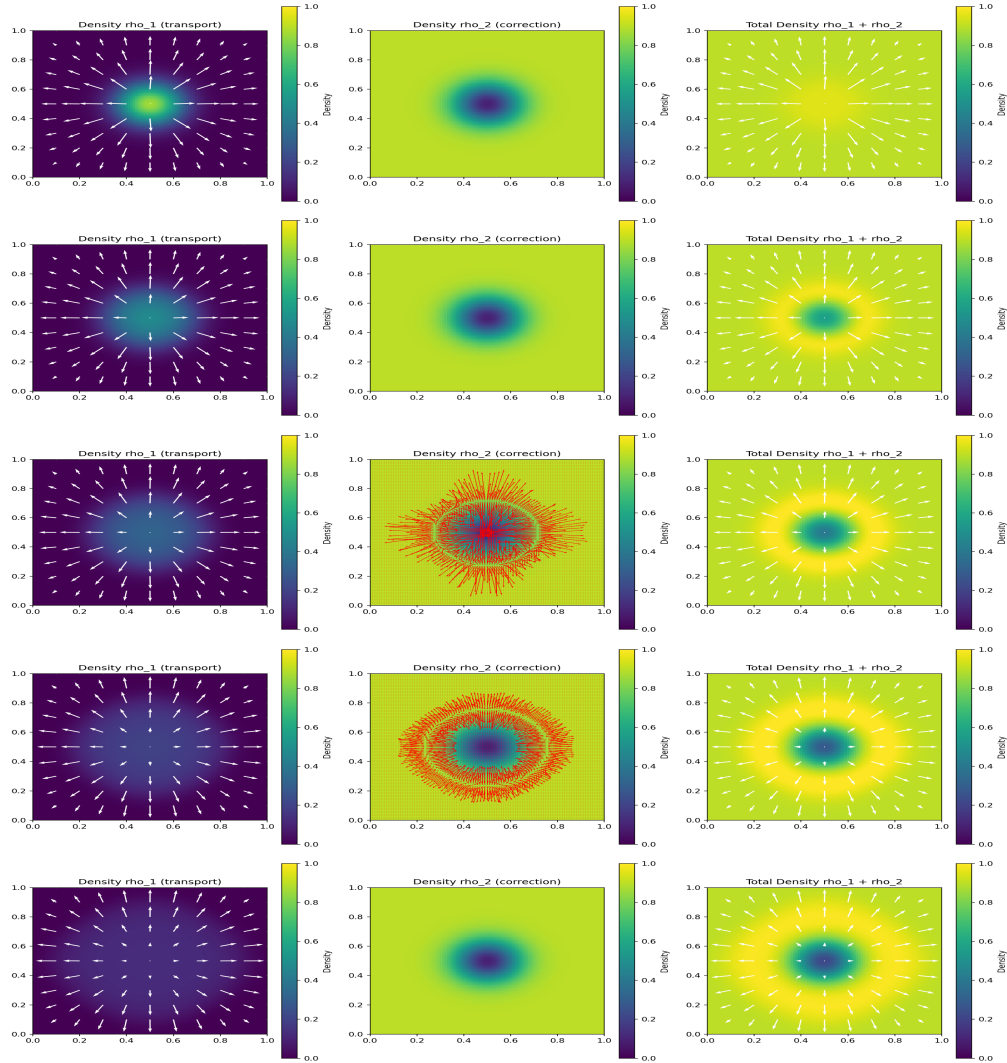


FIGURE 8. We observe a similar behavior to the Dirichlet case with a non-local potential: an undergo phase of congestion followed by stabilization into a non-congested dynamic.

4.3.9. *Example 9:* A scenario similar to Example 5, but employing different initial data distributions for both ρ_1 and ρ_2 .

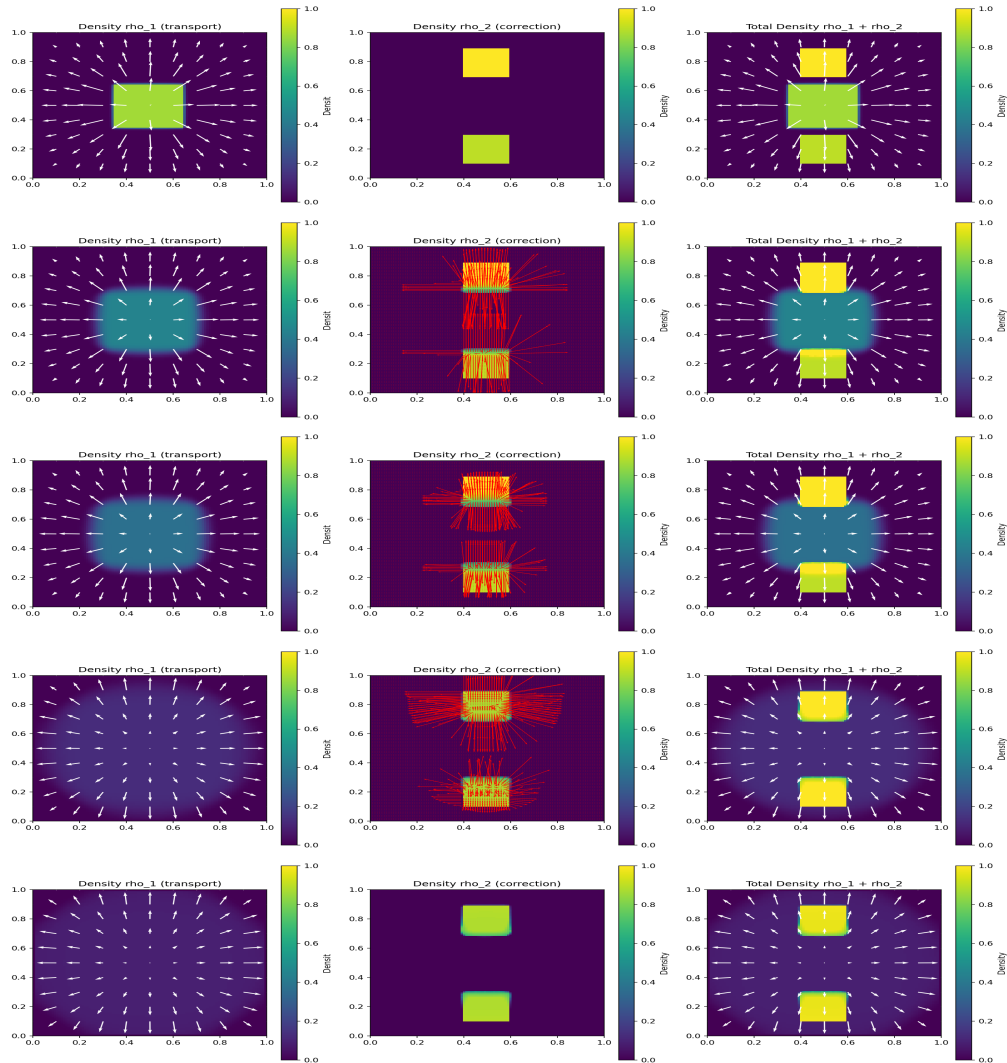


FIGURE 9. Similar outcomes were obtained when applying the method to different datasets, consistent with the findings in Example 8.

Acknowledgments

NI was partially supported by the CNRST of Morocco under the FINCOM program. He is also grateful to the EST of Essaouira for its hospitality. Some numerical results were obtained during SG’s visit to XLIM at the University of Limoges. SG thanks XLIM for their hospitality and acknowledges the support of Cadi Ayyad University.

References

[1] M. Agueh, G. Carlier, and N. Igbida, On the minimizing movement with the 1-Wasserstein distance. *ESAIM Control Optim. Calc. Var.*, **24**(4)(2018) 1415-1427.

- [2] L. Ambrosio, Transport equation and Cauchy problem for BV vector fields. *Invent. Math.*, **158**(2) (2004) 227-260.
- [3] L. Ambrosio and G. Crippa, Existence, uniqueness, stability and differentiability properties of the flow associated to weakly differentiable vector fields, *In Transport equations and multi-D hyperbolic conservation laws, Volume 5 of Lect. Notes Unione Mat. Ital.* (2008) Springer, Berlin 3–57.
- [4] L. Ambrosio, G. Crippa and S. Maniglia, Traces and fine properties of a BD class of vector fields and applications, *Ann. Fac. Sci. Toulouse Math.*, (6), **14**(4) (2005) 527-561.
- [5] B. ANDREIANOV and C. CANCES and A. MOUSSA. A nonlinear time compactness result and applications to discretization of degenerate parabolic–elliptic PDEs. *J. Func. Anal.*, 2017, Vo 273(12), 3633-3670.
- [6] N. Bellomo, L. Gibelli, A. Quaini and A. Reali, Towards a mathematical theory of behavioral human crowds, *Mathematical Models and Methods in Applied Sciences* . **32** (2022) No. 02, 321-358. Open Access <https://www.worldscientific.com/doi/epdf/10.1142/S0218202522500087>
- [7] M. Bertsch, M.E. Gurtin and D. Hillhorst, On interacting populations that disperse to avoid crowding: the case of equal dispersal velocities, *Nonlinear Analysis: Theory, Methods & Applications*, **11**(4) (1987) 493–499.
- [8] G. Bouchitte, G. Buttazzo, and P. Seppecher, Energies with respect to a measure and applications to low dimensional structures, *Calculus of Variations and Partial Differential Equations* Vo. 5, pages 37–54, (1997).
- [9] T. Bord, Highway capacity manual, *204 TRB*.
- [10] J. M. Borwein and D. Zhuang, On Fan’s minimax theorem, *Math. Programming*, **34** (1986), No 2, 232-234.
- [11] F. Boyer, Trace theorems and spatial continuity properties for the solutions of the transport equation. *Differential Integral Equations*, **18**(8) (2005) 891-934.
- [12] J.A Carrillo, K. Craig and Y. Yao, Aggregation-Diffusion Equations: Dynamics, Asymptotics, and Singular Limits, *In: Bellomo, N., Degond, P., Tadmor, E. (eds) Active Particles*, Volume 2. Modeling and Simulation in Science, Engineering and Technology. (2019).
- [13] J.A. Carrillo, S. Fagioli, F. Santambrogio and M. Schmidtchen, Splitting schemes and segregation in reaction cross-diffusion systems, *SIAM J. Math. Anal.* **50**(5)(2018) 5695–5718.
- [14] A. Chambolle, An algorithm for total variation minimization and applications, *J. Math. Imaging Vis.* **20**(1-2) (2004) 89-97.
- [15] A. Chambolle and T. Pock. A first-order primal-dual algorithm for convex problems with applications to imaging. *J. Math. Imaging Vis.*, 40(1):120-145, 2011.
- [16] J. G. Charney, R. Fjortoft and J. Von Neuman, Numerical Integration of the Barotropic Vorticity Equation, *Tellus*. **2**(4) (1980) 237-254.
- [17] G. Crippa C. Donadello and L. Spinolo, Initial–boundary value problems for continuity equations with BV coefficients, *Journal Math. Pure Appl.*, (**102**)**1** (2014) 79-98.
- [18] J. Crank and P. Nicolson, A practical method for numerical evaluation of solutions of partial differential equations of the heat-conduction type, *Mathematical Proceedings of the Cambridge Philosophical Society* **43**(1) (1947) 50-67.
- [19] G. Crippa C. Donadello and L. Spinolo, A note on the initial–boundary value problem for continuity equations with rough coefficients, *Proceedings of HYP2012*, (2012).
- [20] L. De Pascale and C. Jimenez, Duality theory and optimal transport for sand piles growing in a silos, *Adv. Differential Equations*. **20**(9/10) (September/October 2015) 859-886.
- [21] H. Ennaji, N. Igbida and G. Jradi, Prediction-correction pedestrian flow by means of minimum flow problem, *Math. Models Methods Appl. Sci.* **34** (**03**) (2024) 385-416.
- [22] H. Ennaji, N. Igbida and V. T. Nguyen, Augmented Lagrangian methods for degenerate Hamilton-Jacobi equations, *Calc. Var. Partial Differential Equations* , **60**(6) (2021) 0944-2669.
- [23] L. C. Evans and F. Rezakhanlou, A stochastic model for growing sandpiles and its continuum limit, *Comm. Math. Phys.*, **197**(2) (1998) 325-345.

- [24] ME. Gurtin and AC. Pipkin, A note on interacting populations that disperse to avoid crowding, *Quarterly of Applied Mathematics* (1984) 87-94.
- [25] D. Helbing, A mathematical model for the behavior of pedestrians, *Systems Research and Behavioral Science*, **36** (1991) 298-310.
- [26] D. Helbing, P. Molnar, and F. Schweitzer, Computer simulations of pedestrian dynamics and trail formation, **01** (1994) .
- [27] R. L. Hughes, The flow of human crowds, *Annual Review of Fluid Mechanics*. **35** (2003) 169-182.
- [28] N. Igbida, Cross-Diffusion Theory for Overcrowding Dispersal in Interacting Species System, *Preprint* <https://arxiv.org/abs/2403.06464>
- [29] N. Igbida, Equivalent Formulations for Monge-Kantorovich Equation, *Nonlinear Analysis TMA*. **71** (2009), 3805-3813.
- [30] N. Igbida, Evolution Monge-Kantorovich Equation, *J. Differential Equations*. **255 (7)** (2013) 1383-1407.
- [31] N. Igbida and M. Urbano, A granular model for crowd motion and pedestrian flow, *Preprint*. <https://arxiv.org/abs/2402.17361>.
- [32] R. Jordan, D. Kinderlehrer and F. Otto, The variational formulation of the Fokker-Planck equation, *SIAM J. Math. Anal.* **29** (1998) 1-17.
- [33] B. Maury, A. Roudneff-Chupin and F. Santambrogio, A macroscopic crowd motion model of gradient flow type, *Math. Models and Meth. in Appl. Sci.*, **20** (2010), No. 10, 1787-1821.
- [34] S. Mischler, On the trace problem for solutions of the Vlasov equation, *Comm. Partial Differential Equations*. **25(7-8)** (2000) 1415-1443.
- [35] A. Moussa, Some variants of the classical Aubin-Lions Lemma, *J. of Evolution Equations*. **16** (2016) 65-93.
- [36] F. Santambrogio, Optimal Transport for Applied Mathematicians, Progress in Nonlinear Differential Equations and Their Applications. **87** (2015), Birkhauser Basel